Juan Sebastian Giraldo Chavarriaga

Robust and Efficient Voltage Stability Margin Computation using Synchrophasors

CAMPINAS
2015

UNIVERSIDADE ESTADUAL DE CAMPINAS
FACULDADE DE ENGENHARIA ELÉTRICA E DE COMPUTAÇÃO

Juan Sebastian Giraldo Chavarriaga

Robust and Efficient Voltage Stability Margin Computation using Synchrophasors

Cálculo Robusto e Eficiente da Margem de Estabilidade de Tensão usando Sincrofasores

Orientador: Prof. Dr. Carlos A. Castro.

Dissertação de Mestrado apresentada à Faculdade de Engenharia Elétrica e de Computação da Universidade Estadual de Campinas, como parte dos requisitos exigidos para a obtenção do título de Mestre em Engenharia Elétrica, na Área de Energia Elétrica.

ESTE EXEMPLAR CORRESPONDE À VERSÃO FINAL DA DISSERTAÇÃO DEFENDIDA PELO ALUNO Juan Sebastian Giraldo Chavarriaga, E ORIENTADA PELO PROF. DR. Carlos Alberto de Castro Junior.

....
ASSINATURA DO ORIENTADOR

CAMPINAS
2015

Ficha catalográfica
Universidade Estadual de Campinas
Biblioteca da Área de Engenharia e Arquitetura
Elizangela Aparecida dos Santos Souza - CRB 8/8098

Giraldo Chavarriaga, Juan Sebastian, 1989-
G441r Robust and efficient voltage stability margin computation using synchrophasors / Juan Sebastian Giraldo Chavarriaga. – Campinas, SP : [s.n.], 2015.

Orientador: Carlos Alberto de Castro Junior.
Dissertação (mestrado) – Universidade Estadual de Campinas, Faculdade de Engenharia Elétrica e de Computação.

1. Sistemas elétricos de potência. 2. Estabilidade. 3. Spline, Teoria do. 4. Otimização. I. Castro Junior, Carlos Alberto de,1960-. II. Universidade Estadual de Campinas. Faculdade de Engenharia Elétrica e de Computação. III. Título.

Informações para Biblioteca Digital

Título em outro idioma: Cálculo robusto e eficiente da margem de estabilidade de tensão usando sincrofasores
Palavras-chave em inglês:
Electric power systems
Stability
Spline Theory
Optimization
Área de concentração: Energia Elétrica
Titulação: Mestre em Engenharia Elétrica
Banca examinadora:
Carlos Alberto de Castro Junior [Orientador]
Benedito Isaías de Lima Lopes
Daniel Dotta
Data de defesa: 23-07-2015
Programa de Pós-Graduação: Engenharia Elétrica

COMISSÃO JULGADORA - TESE DE MESTRADO

Candidato: Juan Sebastian Giraldo Chavarriaga

Data da Defesa: 23 de julho de 2015

Título da Tese: "Robust and Efficient Voltage Stability Margin Computation Using Synchrophasors (Cálculo Robusto e Eficiente da Margem de Estabilidade de Tensão Usando Sincrofasores)"

Prof. Dr. Carlos Alberto de Castro Junior (Presidente): ____________________

Prof. Dr. Benedito Isaias de Lima Lopes: ____________________

Prof. Dr. Daniel Dotta: ____________________

Abstract

This work presents an efficient method to estimate the Maximum Loading Point and the Voltage Stability Margin of a system in real time with low margin of error. In order to do so, the results of two practical and computationally fast methods based only on Phasor Measurement Units PMUs were used as initial values for a robust and very efficient model-based method that takes advantage of the geometric characteristics of the maximum loading hyperplane and uses the Load Flow with Step Size Optimization to estimate the system's proximity to the point of collapse. Both initializing methods are based on estimated Thevenin Equivalents as seen from load buses using only local measurements. On the other hand, the latter method is based on a set of load flow calculations for specific operating points until the maximum loading point is reached within a defined threshold. The performance of the complete method (combination between the initializing methods and the load flow with step size optimization based method) was tested for some traditional IEEE test systems and for a realistic Brazilian transmission system with more than 4,500 buses.

Keywords: Power system voltage stability, voltage stability margin, phasor measurement units, cubic spline extrapolation, step size optimization.

Resumo

Este trabalho apresenta um método eficiente para estimar o Ponto de Máximo Carregamento e a Margem de Estabilidade de Tensão em tempo real com pequena margem de erro. Para isto, os resultados de dois métodos práticos e computacionalmente eficientes baseados somente em medições fasoriais (PMUs) foram usados como valores iniciais de um outro método baseado no modelo da rede que aproveita as características geométricas do hiperplano de máximo carregamento e usa a técnica de fluxo de carga com otimização de passo para estimar a proximidade do sistema com relação ao ponto de colapso. Ambos os métodos de inicialização são baseados em equivalentes de Thévenin vistos desde as barras de carga usando unicamente medições fasoriais. Por outro lado, este método é baseado em uma serie de cálculos de fluxos de carga para pontos de operação específicos até que o ponto de máximo carregamento seja encontrado dentro de uma tolerância especificada. O desempenho do método completo (combinação entre os métodos de inicialização e o fluxo de carga com otimização de passo) foi testado para alguns sistemas de prova da IEEE e para uma parte do sistema de transmissão Brasileiro com mais de 4,500 barras.

Palavras-chave: Estabilidade de tensão em sistemas de potência, margem de estabilidade de tensão, medição fasorial sincronizada, otimização de passo.

TABLE OF CONTENTS

TABLE OF CONTENTS x

LIST OF FIGURES xvii

LIST OF TABLES xix

1 Introduction 1

1.1 Objectives and Contributions . . . 3

1.1.1 Objectives . . . 4

1.1.2 Contributions . . . 5

1.2 Outline of the Thesis . . . 5

2 Basic Concepts 7

2.1 Power Systems Stability . . . 7

2.2 Voltage Stability . . . 9

2.2.1 Factors contributing to long-term voltage instability . . . 11

2.2.2 Simple example . . . 13

2.2.3 Some methods for voltage stability analysis . . . 16

2.3 Determination of the Thevenin equivalent parameters based on phasor measurements 18

2.4 Load Flow with Step Size Optimization (LFSSO) . . . 20

3 Determination of the Maximum Loading Point (MLP) 25

3.1 Initializing methods . . . 25

3.1.1 Maximum loading point using the Cubic Spline Extrapolation . . . 27

3.1.2 Proposed initializing method 1 . . . 30

3.1.3 Proposed initializing method 2 . . . 31

3.1.4 Example using initializing methods . . . 33

3.2 Performance of Initializing Methods . . . 37

3.2.1 First test . . . 40

3.2.2 Second test . . . 42

3.3 Load Flow with Step Size Optimization for Voltage Stability Analysis . . . 46

3.3.1 Load Shedding Technique 47
3.3.2 Acceptable error margin 49
3.3.3 Example of the use of LFSSO for Voltage Stability 51

4 Proposed Methods **55**
4.1 Proposed Method I: Initializing Method 1 + LFSSO 55
4.2 Proposed Method II: Initializing Method 2 + LFSSO 56
4.3 Example using the Proposed Methods 57
4.4 Tests and Results 59

5 Conclusions and Future work **67**
5.1 Conclusions 67
5.2 Future Work 69
5.3 Publications 70

References **71**

A mi familia, en especial a mi madre Martha Cecilia Chavarriaga,
a quien agradezco su apoyo, comprención y paciencia.

Agradecimentos

Agradeço a minha mãe Martha pelo apoio e paciência.

Ao Prof. Dr. Carlos A. Castro pela confiança depositada em mim e pela indiscutível dedicação e orientação para o desenvolvimento deste trabalho.

Aos meus amigos e companheiros pela colaboração e apoio.

Ao CNPq pelo apoio financeiro durante o desenvolvimento deste trabalho.

LIST OF FIGURES

2.1 Classification of power system stability. 7
2.2 Time scale for voltage stability analyses. Source (TCHOKONTE, 2009) 10
2.3 Typical generator capability curve. Adapted from (JENKINS ET AL., 2008) 12
2.4 On-load tap changer representation. 13
2.5 Two-bus example system. 14
2.6 PV curve for the two-bus example, considering $V_k = 1\,\mathrm{pu}$, $r = 0.067\,\mathrm{pu}$, $x = 0.2\,\mathrm{pu}$. 15
2.7 PV curve for the two-bus example system with polynomial load model. 15
2.8 P-V curve using the continuation power flow. 17
2.9 Thevenin equivalent as seen from bus i. 18
2.10 Parameter space. Adapted from (DE LIMA TAVARES, 2010) 21
3.1 Magnitude of load impedance vs Loading factor. 26
3.2 Maximum loading point with the CSE based on information from bus i. 28
3.3 3-bus system one-line diagram. 34
3.4 Flowchart of the general method. 38
3.5 Daily load curve -– IEEE 14-bus test system. 38
3.6 Interval between phasor measured samples for the second test. 39
3.7 Voltage stability margin and relative error – IEEE 14-bus test system, first test. . . . 40
3.8 Voltage stability margin and relative error – IEEE 118-bus test system, first test. . . 41
3.9 Critical buses – IEEE 30-bus and IEEE 118-bus test systems, first test. 42
3.10 Voltage stability margin and relative error – IEEE 57-bus test system, second test. . 43
3.11 Voltage stability margin and relative error – Brazilian 4,526-bus system, second test. 44
3.12 Critical buses -– IEEE 57-bus test system and Brazilian 4,526-bus, second test. . . 45
3.13 Process to obtain the MLP using the LFSSO. 47
3.14 Acceptable error margin. Adapted from (XAVIER ET AL., 2013) 49
3.15 Illustration of the iterative process. 51
3.16 Behavior of the method LFSSO, 3-bus example system. 53
4.1 Proposed Method I Flowchart. 56
4.2 Proposed Method II Flowchart. 57
4.3 Behavior of the method for the 3-bus example system. 59
4.4 Different loading cases for a particular system. 60

4.5 VSM using different methods. a) 118-bus b) BR 4,526-bus system. 60
4.6 VSM using different methods. a) 30-bus b) 57-bus system. 61
4.7 Number of LFSSO performed. a) 57-bus b) 118-bus. 62
4.8 Number of LFSSO performed. a) 4526-bus b) 30-bus. 62
4.9 MLP process with different initial loading factors. a) IEEE 118-bus b) IEEE 57-bus. 65
4.10 MLP process with different initial loading factors. a) IEEE 14-bus b) BR 4526-bus. 65

LIST OF TABLES

3.1 System bus data 33
3.2 System branch data 33
3.3 Results for bus 2 after running conventional load flows. 34
3.4 Absolute mean error and standard deviation – First test. 41
3.5 Used buses according to the initializing method – First test. 43
3.6 Absolute mean error and standard deviation – Second test. 44
3.7 Used buses according to the initializing method – Second test. 45
4.1 VSM using different calculation methods 63
4.2 MLP using different initializing values 64

1 Introduction

Secure operation of power systems has always been an aspect of high interest and research. The increasing dependence of society on economic, reliable, and safe electricity supplies demands more robust and flexible bulk systems, expected to operate within acceptable operational limits after a wide set of disturbances, that is, to remain stable most of the time. Historically, the stability problem had been mainly focused on transient phenomena, basically because it is a prevailing issue, present in almost every electric system. However, mostly due to the growing number of interconnections and load points, and the interaction of old technologies with new ones, including generation, control devices, among others, studies of different kinds of instabilities such as voltage instability, frequency and inter-area oscillations have become subjects of high interest (KUNDUR ET AL., 2004), (KUNDUR ET AL., 1994), making them an essential part of the security assessment of power systems.

Instability has been recognized as responsible of several blackouts all over the world in the last decades, affecting millions of users and leading to nine-figure losses, such as the blackout occurred in USA and Canada in 2003 (FORCE ET AL., 2004), Brazil in 1999, 2002 and 2009 (ORDACGI FILHO, 2010), and recently in India (2012) affecting more than 600 million people (COMMITTEE ET AL., 2012). These are some examples of the transcendence of this event. Voltage instability is one of the main causes of unplanned electricity outages and is usually manifested as the loss of control on the buses' voltage levels due to an inability of the system to meet the demand. It is also ascribed to system contingencies and to poor local reactive compensation, among others. In fact, the point where the system is no longer able to supply the load, leading to an unstable condition is commonly known as Maximum Loading Point (MLP).

It is well known that voltage stability is essentially a dynamic problem, however, some studies indicate that whether for the slow dynamics of some power equipment, or for poorly known load model dynamics, it can be regarded as a static problem with acceptable accuracy and little computational effort (DOBSON, 1994). Moreover, static approaches allow the analyses of some important features, such as critical buses and stability margins, which are useful parameters in real time environments (LOF ET AL., 1993) and the use of static tools, such as the load flow, demanding less computational effort.

The Newton-Raphson method and its variations are the most used computational routines to solve well-conditioned load flow cases. However, it can present some convergence problems when the system of nonlinear equations results in an ill-conditioned case or for highly loaded systems leading to a bifurcation point, or to an unsolvable case where the solution does not exist. Hence, several different load flow approaches have been presented to overcome this kind of problems, like power flows based on optimal multiplier (IWAMOTO AND TAMURA, 1981), (DEHNEL AND DOMMEL, 1989), (CASTRO AND BRAZ, 1997), (BRAZ ET AL., 2000), (BIJWE AND KELAPURE, 2003), continuation load flow methods (AJJARAPU AND CHRISTY, 1992), (ALVES ET AL., 2000), continuous methods (MILANO, 2009), holomorphic embedding method (TRIAS, 2012), among others.

Traditional static methods for voltage stability assessment, such as successive load flow methods (KESSEL AND GLAVITSCH, 1986) and continuation load flow based methods (AJJARAPU AND CHRISTY, 1992), have been also successfully used in the last decades for actual electric systems, as the case of the Brazilian system (ONS, 2014). However, they can be really time consuming for large interconnected power systems and might not be suitable for real time assessment. Therefore, several approaches based on nondivergent load flow methods, such as (CHAO ET AL., 1995), (BEDRIÑANA AND CASTRO, 2008) using the Load Flow with Step Size Optimization (LFSSO) and on direct methods (CANIZARES AND ALVARADO, 1993), (IBA ET AL., 1991), (DOBSON AND LU, 1993), among others, have been proposed as a more efficient and practical alternative to this conventional methods.

Relatively new technologies for real time assessment, such as Phasor Measurement Units (PMUs) have also been proposed along with static approaches to get synchronized snapshots of the system's operating point in order to provide more updated stability indexes and thus, the possibility to properly react under probable insecure situations (VU ET AL., 1999), (HAQUE, 2003), (VERBIC AND GUBINA, 2004), (SMON ET AL., 2006), (PARNIANI ET AL., 2006), (CORSI AND TARANTO, 2008), (GLAVIC AND VAN CUTSEM, 2011) and (DAS, 2014). PMUs are considered one of the most important measuring devices in the future of power systems. They are capable of measuring system's variables, such as voltages and currents, directly with a GPS-synchronized time stamp (HOLBERT ET AL., 2005), so besides the magnitudes, system phase angles can also be transmitted at very high rates (up to 120 frames per second). This is maybe one of their most remarkable characteristics since it makes them useful for both dynamic and static assessments as explained in (YANG AND LIU, 2000), (PHADKE, 2002) and (HOLBERT ET AL., 2005).

Actually, synchronized measurements have been used to estimate voltage security indexes since mid-80's (KESSEL AND GLAVITSCH, 1986), however it was not until a decade after that a

Voltage Stability Margin (VSM) was first proposed using PMUs (TUAN ET AL., 1994), (GUBINA AND STRMCNIK, 1995). Since then, several methodologies have used similar concepts to estimate the system's proximity to the MLP (VU ET AL., 1999), (VERBIC AND GUBINA, 2002), (SMON ET AL., 2006), (CORSI AND TARANTO, 2008), (VOURNAS AND VAN CUTSEM, 2008), (SU ET AL., 2012) and (LEELARUJI ET AL., 2012), in fact, there are several experiences of PMUs systems working in the Brazilian transmission system as the ones exposed in (DECKER ET AL., 2006) and (DECKER ET AL., 2011) and in New Zealand (PENG ET AL., 2011). Although nearly all of them are based on Thevenin Equivalents (TEs) as seen from every load bus, there are also other kinds of approximations such as in (LEELARUJI ET AL., 2012), where the estimation of the Jacobian matrix terms (sensitivities) is made using phasor measurements, in (SMON ET AL., 2006) where the Tellegen's theorem is used to estimate a local voltage stability index or in (VOURNAS AND VAN CUTSEM, 2008) by monitoring the distribution voltages controlled by load tap changers on bulk power delivery transformers, just to mention a few. Nonetheless, TE based methods have an important advantage related to their simplicity and minimal computational burden, making them more suitable for real time applications.

1.1 Objectives and Contributions

Fast assessment of power systems' voltage stability in real time operation is a crucial matter from the control center's point of view. Updated operational information and appropriate tools to infer the meaning of the measured data could be enough to know whether a system can maintain acceptable voltage levels after being subject to disturbances and to take appropriate actions accurately. Methods based on PMUs like (SU ET AL., 2012) have shown to be a good alternative to estimate system's VSM, mainly because of their simplicity and computational efficiency, since they are independent from network's model and based only on local measurements, which makes them a really good option for real time operation. Nevertheless, these methods have presented some drawbacks especially under light load scenarios and under certain operational conditions, such as significant system variations between samples, errors in the estimation of the TE, among others. This has led this kind of approaches to be used as an additional part of more robust ones.

On the other hand, depending on the system's characteristics, conventional load flow methods may present convergence problems or even diverge, in spite of being on a feasible operating point. As stated before, several approaches have been proposed in order to overcome this kind of ill-conditioning problems. Moreover, it is expected that a load flow method be able to provide additional information on the iterative process so that the voltage stability analysis method can take advantage of it. Some nondivergent methods using the LFSSO technique to estimate the system's MLP as (BEDRIÑANA AND CASTRO, 2008), (TAVARES ET AL., 2010), (TAVARES ET AL., 2011) and (XAVIER ET AL., 2013) take advantage of the additional information provided by the so-called optimal multiplier, in addition with a load curtailment technique and showed excellent performance for voltage stability analysis. Still, they need an initial estimate value for the MLP either in the feasible or infeasible region.

1.1.1 Objectives

The main objective of this work is to obtain an efficient and robust method for a model-based assessment of long term small-disturbance voltage stability. Two proposed PMU-based model-free methods are used as initializing values of a more robust method based on the LFSSO technique (XAVIER ET AL., 2013). The drawbacks of the initializing methods can be overcome by using a model-based method and the number of LFSSO is minimized using appropriate initializing values. To reach the main objective some tasks must be performed:

(1) Implementation of a power systems voltage stability assessment method using Thevenin Equivalents obtained through synchronized measurements in load buses, hereafter referred to as initializing method.

(2) Evaluation of the performance of the initializing method compared with well-known methodologies, such as the continuation power flow (AJJARAPU AND CHRISTY, 1992), and its behavior towards its application in real time environments.

(3) Implementation of a power systems voltage stability assessment method based in the Load Flow with Step Size Optimization technique, such as (XAVIER ET AL., 2013).

(4) Implementation of a power systems voltage stability assessment method using the methodology developed in (1) as initializing values for the method in (3).

(5) Evaluation of the performance of the proposed method compared with well-known methodologies, such as the continuation power flow (AJJARAPU AND CHRISTY, 1992).

1.1.2 Contributions

The basic contributions of this work are:

- Two initializing methods based on synchronized phasor measurements to estimate the system's proximity to the MLP are introduced, presenting some interesting characteristics. The first one allows finding the weakest bus of the system for a certain operation point. The knowledge of this kind of information would be interesting for the optimization of the quantity of information that has to be computed by the method, since analysis of relatively irrelevant data could be avoided. The second initializing method presents a similar advantage in terms of potential computed information, however, the main difference is that it finds not only the weakest bus but a set of weakest buses, the most critical buses within a specified threshold.
- The use of initializing methods for the LFSSO based method to find the VSM is also a new feature compared with previous works, since their initial values were set arbitrarily, basically to show the robustness of the method. The use of initializing values showed a significant reduction on the number of LFSSO needed to get the desired solution.

1.2 Outline of the Thesis

This thesis starts in *Chapter 2* with a review of some crucial concepts for the understanding of the problem, such as its definition and classification, some factors contributing to voltage instability, classic methods to calculate system's proximity to the collapse point and finally the basic concepts used by the methods proposed. It is followed by the explanation and evaluation of the so called Initializing Methods and the use of the LFSSO for voltage stability assessment in *Chapter 3*. In *Chapter 4* are exposed the proposed methods, a basic example showing the motivation of its use and the results obtained using several test systems and a real transmission system. Finally in *Chapter 5* summarizes the work done and ends with some ideas for future work.

2 Basic Concepts

This chapter presents a brief definition and classification of power system's stability, a small revision of some classic methods used for voltage stability assessment, and finally the basic theory behind the proposed methods.

2.1 Power Systems Stability

In general, the term *stability* is related to the characteristic of an element, object, system, etc. to remain in an equilibrium estate after suffering a disturbance on its normal operation. For electric power systems this definition does not change too much and has been commonly accepted as the ability of a power system to regain a state of operating equilibrium with most of its system variables bounded after being subjected to disturbances (KUNDUR ET AL., 2004). Since power systems are highly nonlinear problems and their stability depends on the initial operating condition as well as on the nature of the disturbance, the stability problem can be classified into several different subproblems, depending on different factors like its physical nature, the size of the disturbance, the dynamic behavior of the implied elements, etc. This facilitates the problem identification and the development and use of appropriate analysis methods. Even though some of the definitions can overlap with others, power system stability is basically divided into three main categories, namely rotor angle stability, frequency stability and voltage stability, as shown in Figure 2.1.

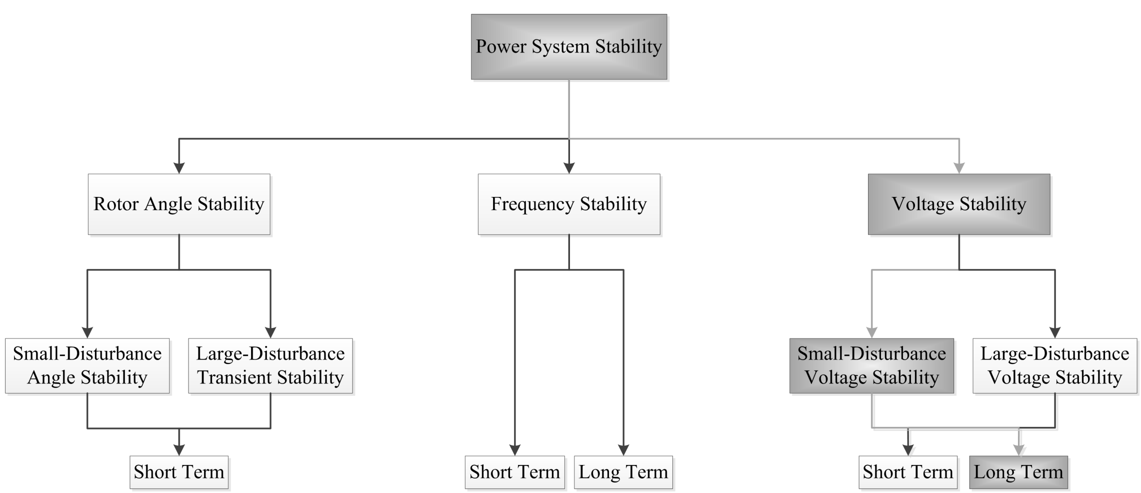

Figure 2.1: Classification of power system stability.

Rotor angle stability has been defined as the ability to maintain or restore equilibrium between the electromagnetic torque (synchronizing and damping components) and the mechanical torque of each synchronous machine in the system (VAN CUTSEM AND VOURNAS, 1998). It is divided in small-disturbance (small-signal) rotor angle stability and transient stability. The small-signal stability is concerned with the ability of the power system to maintain synchronism under small disturbances, such as load and generation normal variations, being commonly attributed to a lack of damping torque. On the other hand, transient stability is related to severe disturbances such as faults in transmission lines or in transformers and is usually presented as a lack of synchronizing torque commonly known as first swing stability, even though it could also happen after rotor's angle large variations beyond the first swing (KUNDUR ET AL., 1994). Both are categorized in the short term time frame (3–20 seconds) which is the time scale for electromechanical dynamics studies. This time frame also includes interarea oscillation.

Frequency stability is the ability of a power system to compensate for a power unbalance. It is concerned with the balance between generation and load and related with the angular velocity of generation synchronous machines. Under normal operating conditions, the mechanical torque, produced by water, steam, wind, etc, and the electrical torque (generator output) are considered equal or within the system's acceptable frequency variations. However, if a disturbance occurs in the system, generators may present changes on their angular velocities and hence in the system's frequency. This kind of instability is generally in the form of frequency swings and typically after a great loss of generation power (TCHOKONTE, 2009), and also associated with inadequacies in equipment responses, poor coordination of control and protection equipment, or insufficient generation reserve (KUNDUR ET AL., 2004). Depending on the control actions performed, it is generally classified as short term for primary and secondary control actions, and long term for tertiary control (generation re-dispatch).

Finally, voltage stability occurs when the load attempts to step beyond the capability of the combined transmission and generation system, this is, crosses the Maximum Loading Point (MLP), leading to an uncontrollable drop or rise of bus voltages. Since the main objective of this work relates long term small-disturbance voltage stability, a deeper discussion and explanation of the phenomena will be done in the next section.

2.2 Voltage Stability

Voltage instability is manifested in the form of uncontrollable bus voltage levels after the system is subjected to a disturbance related with load or generation. Thus, a system is considered stable if the voltages at all buses remain within bounds. Voltage stability depends on the balance between generation and load, and appears on heavily loaded systems with low reactive reserves or when subjected to contingencies, disturbances or unforeseen load increase. This clarification has to be done since rotor angle instability is also sometimes responsible for bus progressive voltage drops (KUNDUR ET AL., 1994). Voltage stability is considered a load driven problem, mainly because after a disturbance load tend to be restored, whether by the adjustment of slip in motors, action of distribution regulators, on load tap changers (OLTCs), among others, increasing the reactive power consumption leading to a further voltage reduction, resulting in a vicious cycle until the system reaches an unstable operation point (VAN CUTSEM AND VOURNAS, 1998).

Depending on the severity of the disturbance, voltage stability can also be divided in two categories, namely small and large-disturbance. As for angle stability, small-disturbance voltage stability refers to small perturbations, such as normal variations in generation and load. Since the operating point does not change too much, several assumptions can be made and the equation system can be linearized around an operating point allowing the use of steady state analysis tools typically based in load flows or in eigenvalues and eigenvectors techniques, thus providing information regarding the sensitivity or degree of instability, participation factors and reducing the computation time (MORISON ET AL., 1993). However, static analyses do not consider some nonlinear effects like tap controls, thermostatically controlled loads, induction motors, etc. Large-disturbance voltage stability analyses the response of the system to large disturbances like faults, loss of generation or circuit contingencies (KUNDUR ET AL., 2004). Similarly to angle stability, analyses must be performed in the time domain, since the dynamics of some devices such as motors, OLTC and generator field-current limiters must be evaluated. The study period of interest may extend from a few seconds to tens of minutes.

Short term voltage stability analysis involves fast recovering load components such as induction motors, electronically controlled loads, and HVDC converters. They tend to restore power consumption in a short time period after a disturbance, so its time scale is similar to that used for rotor angle stability. For long term, slower acting equipment dynamics are considered, such as OLTC, thermostatically controlled loads, and generator current limiters. Its study period of interest may extend to several or many minutes. It is usually attributed to the attempts of load to step beyond the capability of the combined transmission and generation system, that is, the Maximum Loading Point. Since slower dynamics are taken into account in this kind of study, static approaches have been widely used with success, such as successive load flow methods (KESSEL AND GLAVITSCH, 1986), continuation load flow based methods (AJJARAPU AND CHRISTY, 1992), non-divergent load flow methods using the LFSSO (CHAO ET AL., 1995) and (BEDRIÑANA AND CASTRO, 2008), and direct methods like (IBA ET AL., 1991), (DOBSON ET AL., 1991), (CANIZARES AND ALVARADO, 1993) and (DOBSON AND LU, 1993); however if dynamic assessment is necessary, several approaches have also been developed and some of them are explained in (GAO ET AL., 1996), (VAN CUTSEM, 2000) and (DASGUPTA ET AL., 2012). Finally, Figure 2.2 shows the dynamic range of the main components, control and actions of the system that may play an important role in voltage stability are shown, divided in short-term and long-term time frames.

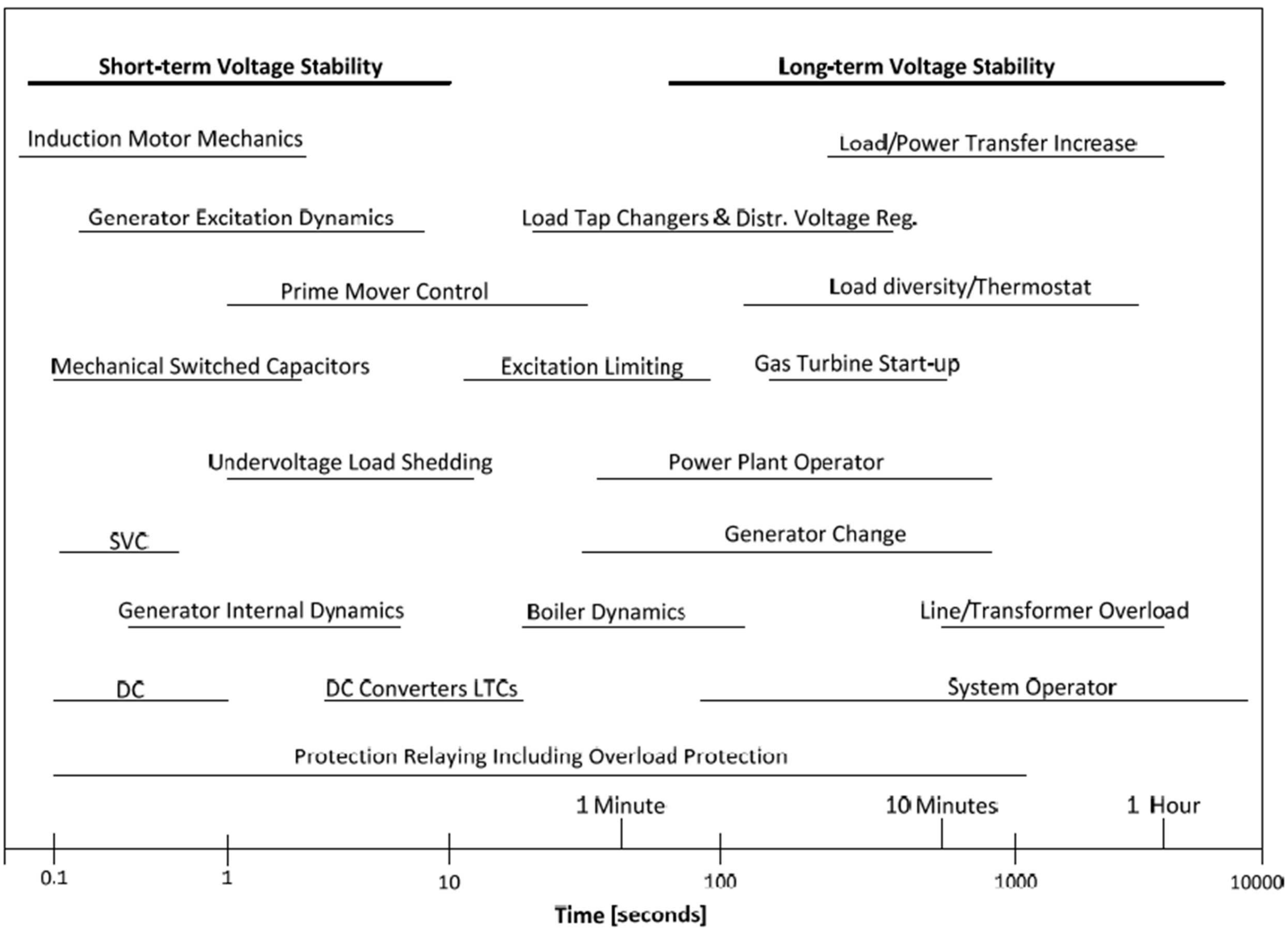

Figure 2.2: Time scale for voltage stability analyses. Source (TCHOKONTE, 2009)

2.2.1 Factors contributing to long-term voltage instability

It is well known that voltage instability is a local problem that spreads out, affecting the whole system or a part of it if timely and accurate correction actions are not taken. Voltage instability is a natural dynamic phenomenon, however, steady state studies are ideal for bulk systems, either if a large number of contingencies must be analyzed or if real time assessment in the long-term frame is needed (REPO, 2001). Dynamics of fast devices like induction motors, excitation control of synchronous machines, FACTS and HVDC control, etc. are not of high interest in this time frame since, as mentioned above, all dynamics are supposed to be over and it is considered that control devices have already acted. Hence, the system's model can be much the same of the one used for load flow studies. Therefore, some slow devices and controls used in power systems, such as tap-changing transformers, passive compensation devices, characteristics of loads and generator current limiters are essential for the study of voltage stability in long-term.

- **Capability of synchronous generators** Reactive power injection from synchronous machines, especially from generators, is considered as one of the primary controls for voltage stability in power systems since most of the reactive power reserves are managed there. Voltage instability is highly related to the power capacity of transmission lines since power must flow from generators to loads in order to meet both active and reactive power demand. If the reactive power demand increases beyond the sustainable capacity of the reactive power resources and transmission corridors the system stability might be threatened (TCHOKONTE, 2009). Thus, the operational limitations of generators, which are basically the armature maximum current, field maximum current (over-excitation limit) and under-excitation limit, must be taken into account.

  A typical generator capability curve in the P-Q diagram is shown in dashed lines in Figure 2.3. It can be seen that operational limits are nonlinear since they depend on the machine's parameters, like maximum output power, synchronous reactances, etc. If too much detail in the generator's model is not required, as for static approaches, linear limits are commonly used, such as those represented by continuous lines in Figure 2.3.

- **Voltage dependency of loads** Load modeling is a very important research area. It has been shown that an inaccurate load modeling can impact significantly voltage stability analyses, so improving load models is of great importance (PRICE ET AL., 1993). Power consumption and voltage recovery depend on the load's nature, for example, the behavior of electric heaters

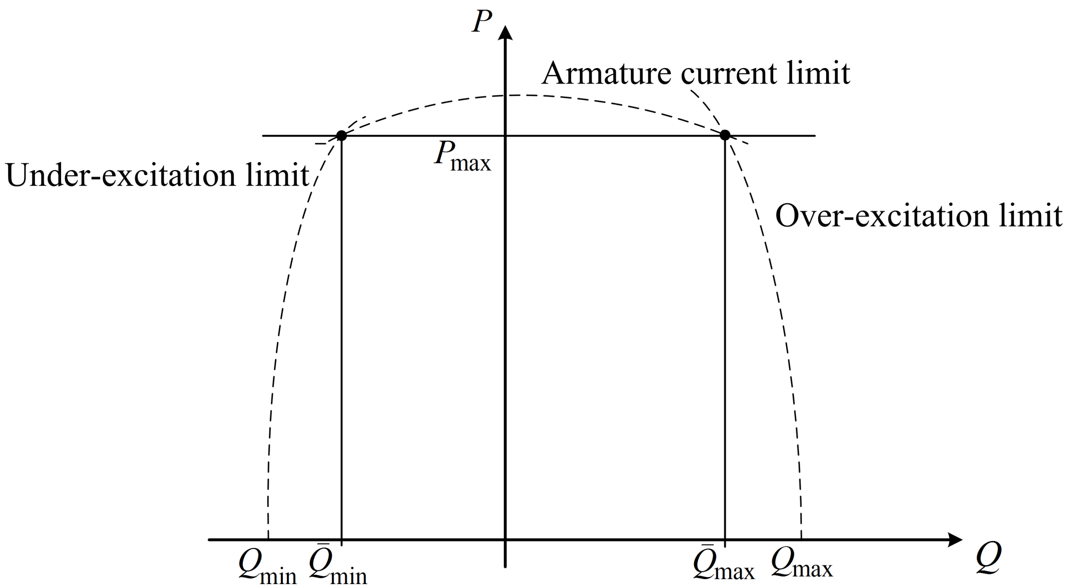

Figure 2.3: Typical generator capability curve. Adapted from (JENKINS ET AL., 2008)

under voltage variations is not the same as of induction motors, so different models must be developed in order to represent their particular voltage dependence. However, modeling of loads is still a difficult task mostly because of the lack of precise information on the composition of the load and the difficulty of testing real systems to identify load models (ROMERO NAVARRO, 2002). Depending on the type of analysis, models can be classified in static or dynamic. Static load models characterize the power consumption as an algebraic function of the voltage magnitude, i.e. it is only dependent on voltage and not on time, as for example an incandescent light bulb model. On the other hand, dynamic load models depend both on voltage and time resulting in differential equations (PAL, 1994), such as the torque in an induction motor that is a function of slip and hence of time. The static voltage dependence is usually represented by an exponential (2.1) or a polynomial (2.1) model, also known as ZIP model. Some typical parameter values for different load types can be found in (HAJAGOS AND DANAI, 1998).

$$P = P_0 \left(\frac{V}{V_0} \right)^{\alpha}, \qquad Q = Q_0 \left(\frac{V}{V_0} \right)^{\beta} \tag{2.1}$$

$$P = P_0 \left[z_p \left(\frac{V}{V_0} \right)^2 + i_p \left(\frac{V}{V_0} \right) + p_p \right], \qquad Q = Q_0 \left[z_q \left(\frac{V}{V_0} \right)^2 + i_q \left(\frac{V}{V_0} \right) + q_q \right] \tag{2.2}$$

- **On-load tap changers** Automatic voltage changes in transformers are performed by controlling the turn ratio between primary and secondary windings, generally to control one of its terminal buses or a remote bus. A transformer tap is a connection point somewhere along the winding that allows a different number of turns. When this variation is made without interrupting the power flow through its terminals, the equipment is called an on-load tap changer (OLTC). Tap changes affect the reactive power flowing through the primary and secondary windings. For example, when the voltage is too low in the secondary of a distribution transformer, the action of the tap controller drives the voltage back to acceptable values, nevertheless, the reactive power flowing from the transmission to the distribution network increases, what might be dangerous if the system is close to the MLP or under a disturbance. A generalized representation of an in-phase OLTC can be made through a π equivalent circuit as in Figure 2.4 (NEDIC, 2002), where y_{km} takes into account real power losses and magnetic field leakage, and t represents the tap position.

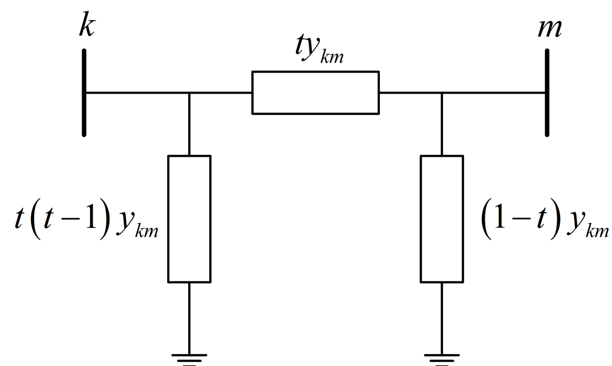

Figure 2.4: On-load tap changer representation.

2.2.2 Simple example

Figure 2.5 shows a simple power system consisting of infinite bus k, a transmission line modeled as a series impedance $r + jx$ and a load $P + jQ$ connected to bus m.

Applying Kirchhoff's laws results in

$$\widetilde{V}_k = \widetilde{V}_m + (r + jx)\left(\frac{P + jQ}{\widetilde{V}_m}\right)^* . \tag{2.3}$$

From (2.3) one gets

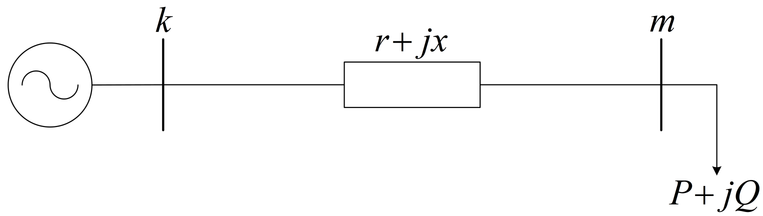

Figure 2.5: Two-bus example system.

$$V_m^4 + V_m^2 \left[2\left(rP + xQ\right) - {V_k}^2\right] + \left(rQ - xP\right)^2 + \left(rP - xQ\right)^2 = 0\,. \tag{2.4}$$

Equation (2.4) is biquadratic and can be written as $ax^2 + bx + c = 0$ where $x = V_m^2$, so the solution can be obtained by

$$V_m = \left[\frac{-b \pm \sqrt{b^2 - 4ac}}{2a}\right]^{1/2}\,. \tag{2.5}$$

It should be noted that the solution of (2.5) results in two positive and two negative answers, from which the negative ones are neglected because they do not have a physical meaning. The two remaining answers correspond to voltage magnitudes in the so-called PV curve. In the bifurcation point both positive answers become equal, so the MLP can be easily found by solving $b^2 - 4ac = 0$, assuming that $Q_{max} = P_{max}\left(\frac{Q}{P}\right)$ for constant power factor. Figure 2.6 shows the well-known PV curve for the example system using different load power factors for constant power load model.

It can be seen that, depending on the power factor, the PV curve takes different shapes and the MLP also changes. For lagging power factors the maximum deliverable power is considerably less than for unity power factor, for example. This shows the relationship between the local reactive power consumption and the MLP. If local reactive compensation is taken into effect, as in the case of the leading power factor, the bifurcation point is increased, since less reactive power has to be transferred from the generator to the load and the voltage drop in the transmission line is reduced.

Voltage instability is largely affected by the load characteristics, as mentioned before and explained in (MILOSEVIC AND BEGOVIC, 2003). Figure 2.7 illustrates this aspect. It was obtained using the polynomial load model or ZIP static model explained in section 2.2.1, which is a

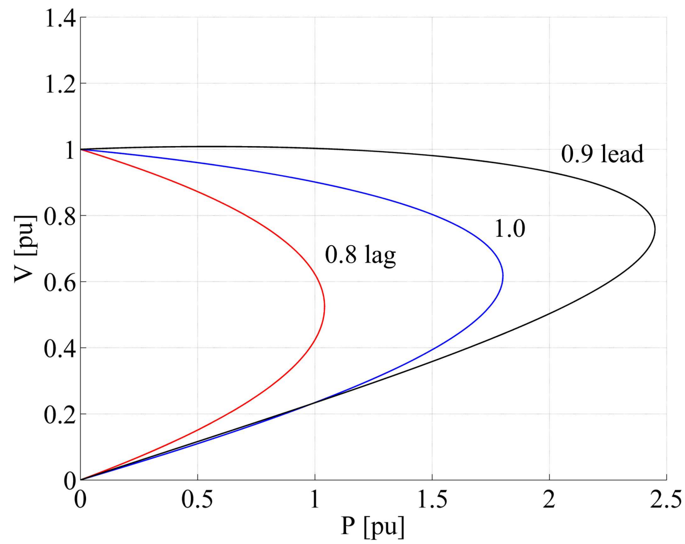

Figure 2.6: PV curve for the two-bus example, considering $V_k = 1$ pu, $r = 0.067$ pu, $x = 0.2$ pu.

combination of constant impedance, constant current, and constant power for the two-bus example system used before with $P_0 = 50$ MW and $Q_0 = 20$ MVAr and assuming constant power factor.

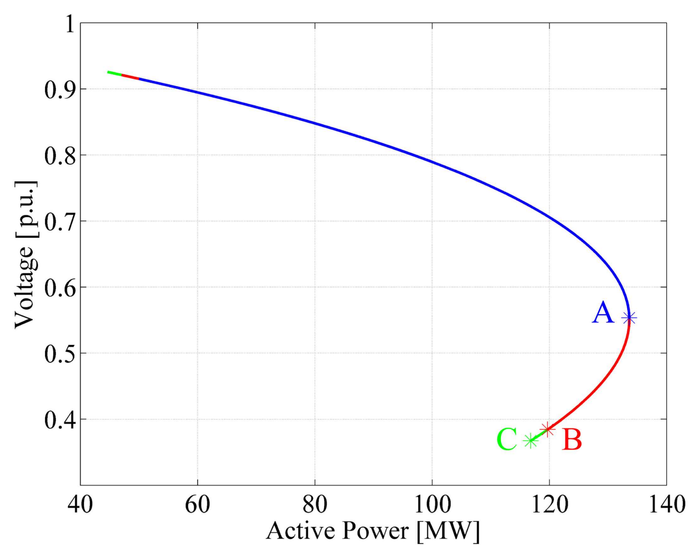

Figure 2.7: PV curve for the two-bus example system with polynomial load model.

Point A in Figure 2.7 represents the system's MLP. It can be seen that it is independent on the used model and lies on the nose of the PV curve for a purely constant power load ($p_p = 1$) coinciding with the critical operating point. On the other hand, the critical operating point remains stable beyond the MLP when modeling loads with impedance and constant current components, as seen in points B ($p_p = 0.25$ and $i_p = 0.75$) and C ($p_p = 0.25$ and $z_p = 0.75$). This actually shows that the most critical case is when all loads in the system are purely constant power loads. This aspect has been discussed in (PRICE ET AL., 1993).

2.2.3 Some methods for voltage stability analysis

The literature contains several voltage stability methods to calculate the MLP and the system's proximity to it as in (CANIZARES ET AL., 2002), (CANDELO ET AL., 2008) and (GLAVIC AND VAN CUTSEM, 2011). Some are more commonly used than others due to their effectiveness, simplicity or computation requirements and are briefly explained in this section.

- **Minimum singular value of the Jacobian matrix**

  The minimum singular value is an index to quantify the proximity to the MLP. It was first proposed in (TIRANUCHIT AND THOMAS, 1988) and later improved in (LOF ET AL., 1992). It is based on the singular value decomposition of matrix $\mathbf{A}$ of a linear system $\mathbf{A}x = b$. In our case this linear system is the linearized load flow equations system and the matrix is the Jacobian matrix. This procedure analyses the influence of small changes on active and reactive power injections $[\Delta P \quad \Delta Q]^T$ to the change of bus angles and voltage magnitudes $[\Delta\delta \quad \Delta V]^T$. The solution using the singular value decomposition is shown in (2.6).

$$\begin{bmatrix} \Delta\delta \\ \Delta V \end{bmatrix} = \mathbf{J}^{-1} \begin{bmatrix} \Delta P \\ \Delta Q \end{bmatrix} = \left(\mathbf{U\Sigma V}^{\mathrm{T}}\right)^{-1} \begin{bmatrix} \Delta P \\ \Delta Q \end{bmatrix} = \mathbf{V\Sigma}^{-1}\mathbf{U}^{\mathrm{T}} \begin{bmatrix} \Delta P \\ \Delta Q \end{bmatrix}, \tag{2.6}$$

  where $\mathbf{J}$ is the Jacobian matrix, $\mathbf{U}$ and $\mathbf{V}$ are orthonormal matrices and $\mathbf{\Sigma}$ is a diagonal matrix containing the singular values of $\mathbf{J}$. The minimum singular value is a measure of how close to singularity the Jacobian matrix is. If this value is zero, it means that the matrix is singular at that point so its inverse does not exist. Other useful information can be derived from this analysis, such as critical areas and components.

- **Continuation Power Flow**

  Its purpose is to find a sequence of power flow solutions for several given load scenarios, overcoming the ill-conditioning and eventually the singularity of the power flow Jacobian as the network gets more stressed (IBSAIS AND AJJARAPU, 1996). The technique solves the power flow equations using a locally parameterized continuation algorithm employing a predictor-corrector scheme. The path is set by a prediction step based on a known solution using, for instance, a tangent predictor (AJJARAPU AND CHRISTY, 1992). If step size and path direction are chosen appropriately, it can predict the next P-V curve solution. An illustration of a P-V curve using the continuation power flow is shown in Figure 2.8.

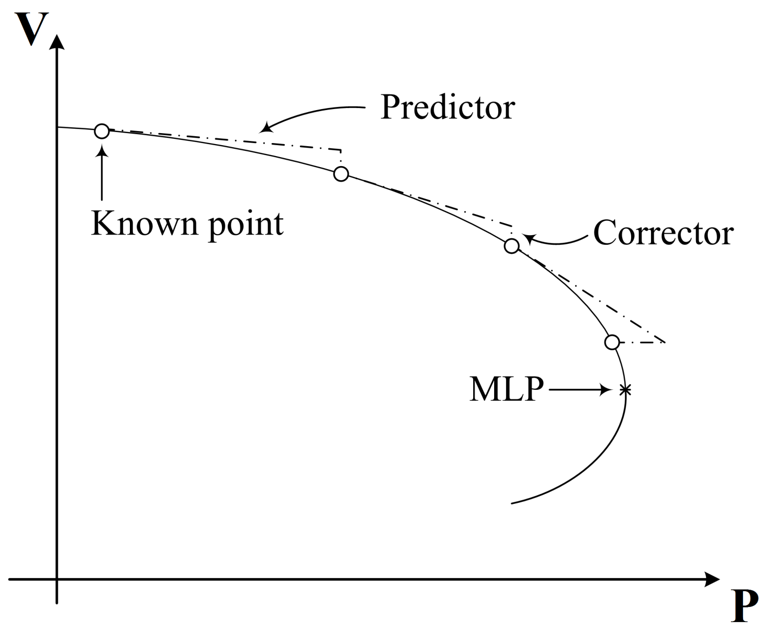

Figure 2.8: P-V curve using the continuation power flow.

This method easily indicates whether or not the system has violated the MLP, however the exact critical point requires a variable step size around the maximum point, leading to a high number of iterations if low thresholds are needed. This is why some simpler predictors, such as the secant predictor, and step size controls have also been proposed sacrificing accuracy but requiring less computation (CHIANG ET AL., 1995).

- **Point of collapse method**

  The point of collapse is a direct method based on bifurcation theory of nonlinear systems and the singularity of the Jacobian matrix to estimate the distance in state space to the MLP (CAÑIZARES ET AL., 1992). The method is used to solve the singularity point of load flow equations by adding some additional equations describing conditions of singularity. Therefore, the resulting system of equations has a solution even if the original load flow Jacobian matrix is singular. One of its biggest drawbacks is that it might not be too accurate if a distant initial point is set, especially if few generators have reached their reactive power limits (VAN CUTSEM AND VOURNAS, 1998). When compared to the continuation power flow, it showed to be as accurate and in fact, have better characteristics in terms of computational time (CANIZARES AND ALVARADO, 1993). On the other hand, continuation methods showed to produce additional and complementary information.

- **Optimization methods**

  These methods are based on the eventual elimination of the Jacobian matrix singularity through a modification in the conventional Newton-Raphson load flow method. They can be similar to direct methods or based on the continuation power flow, but using optimization techniques (IRISARRI ET AL., 1997). There are several techniques that can be used to solve the problem, such as sequential quadratic programming (OBADINA AND BERG, 1988), particle swarm optimization (YOSHIDA ET AL., 2000), nonlinear programming (ZARATE ET AL., 2006) among others. Nevertheless, interior point methods showed to be a better alternative due to the problem's nature (IRISARRI ET AL., 1997) and (WANG ET AL., 1998). However, the computational effort taken by the algorithm for building and factorizing the augmented Hessian matrix makes them not suitable for real time assessment.

2.3 Determination of the Thevenin equivalent parameters based on phasor measurements

Assuming that there are PMUs installed at all load buses, each one of them can be represented as being connected to a Thevenin equivalent that represents the rest of the network, as shown in Figure 2.9 for bus i.

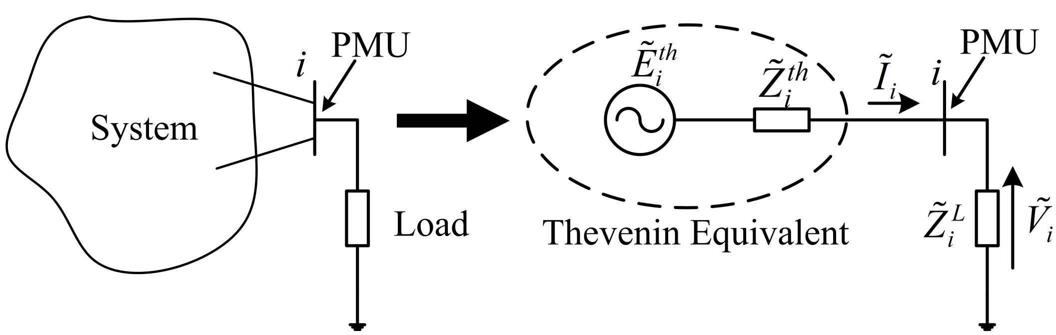

Figure 2.9: Thevenin equivalent as seen from bus i.

Using the PMUs' measurements, phasors $\tilde{V}_i(k)$ and $\tilde{I}_i(k)$ can be obtained in real time for sampling cycle *k*. Then, it is straightforward to find the load's impedance $\tilde{Z}_i^L(k)$ and power $\tilde{S}_i^L(k)$, where symbol ~ indicates a complex number.

It is important to highlight that all measurements coming from PMUs must be previously processed and filtered, since real time measurements inherently carry the effects of switching devices, unexpected events on measured data, environment's behavior, noise, outliers among other factors that can cause errors when estimating the Thevenin equivalent. Some filtering methods, as the one used in (LEELARUJI ET AL., 2012) to smooth the signal data before calculating the voltage sensitivities, or in (ABDELKADER AND MORROW, 2012) in order to facilitate the online estimation of the Thevenin equivalent, can be used to overcome this drawbacks.

At least two consecutive or very close samples for different operating points are needed to determine the parameters of the TE (SU ET AL., 2012). Applying the second Kirchhoff's law to the base circuit of Figure 2.9 for sampling cycles $(k-1)$ and k one gets

$$\begin{aligned} \tilde{E}_i^{th}(k-1) &= \tilde{Z}_i^{th}(k-1)\tilde{I}_i(k-1) + \tilde{V}_i(k-1) \text{ and} \\ \tilde{E}_i^{th}(k) &= \tilde{Z}_i^{th}(k)\tilde{I}_i(k) + \tilde{V}_i(k)\ , \end{aligned} \tag{2.7}$$

leading to a linear system with two equations and four unknowns. In order to solve this problem, it is assumed that there are no topology changes nor significant variations in lines' parameters and that there are no significant voltage and frequency variations in voltage sources between samples. These assumptions result into constant TE parameters during the sampling period, that is, $\tilde{E}_i^{th}(k-1) = \tilde{E}_i^{th}(k) = \tilde{E}_i^{th}$ and $\tilde{Z}_i^L(k-1) = \tilde{Z}_i^L(k) = \tilde{Z}_i^L$, as discussed in (SU ET AL., 2012), (VU ET AL., 1999), (SMON ET AL., 2006) and (ABDELKADER AND MORROW, 2012), leading to

$$\begin{bmatrix} 1 & -\tilde{I}_i(k) \\ 1 & -\tilde{I}_i(k-1) \end{bmatrix} \begin{bmatrix} \tilde{E}_i^{th} \\ \tilde{Z}_i^{th} \end{bmatrix} = \begin{bmatrix} \tilde{V}_i(k) \\ \tilde{V}_i(k-1) \end{bmatrix}. \tag{2.8}$$

After solving the linear system of equations $\mathbf{A}x = \mathbf{B}$ the parameters of the TE can be expressed as

$$Z_i^{th} = \frac{\tilde{V}_i(k-1) - \tilde{V}_i(k)}{\tilde{I}_i(k) - \tilde{I}_i(k-1)}, \text{ and} \tag{2.9}$$

$$\tilde{E}_i^{th} = \frac{\tilde{V}_i(k-1)\tilde{I}_i(k) - \tilde{V}_i(k)\tilde{I}_i(k-1)}{\tilde{I}_i(k) - \tilde{I}_i(k-1)} \tag{2.10}$$

As said before, at least two samples for different operating points are needed to determine the parameters of the TE. If more samples must be used, some adjustments have to be performed, as explained in (HAQUE, 2003). It should be noticed that measurements are not always precise and the Thevenin parameters sometimes drift, between others, due to the system's changing conditions. Thus, parameters must be calculated repeatedly using the most updated available measurements in order to get a good representation of the rest of the network, however, there has to be a difference between the used samples in order to obtain useful values.

2.4 Load Flow with Step Size Optimization (LFSSO)

The Load Flow with Step Size Optimization (LFSSO) is a nondivergent power flow that considers the determination of the step size in the direction of the mismatch vector as a nonlinear programming problem, expanding the load flow equations up to the second order terms in Taylor series. It was first proposed in (IWAMOTO AND TAMURA, 1981) considering voltages in rectangular coordinates. Later in (CASTRO AND BRAZ, 1997) it was extended for voltages in polar coordinates too, facilitating its application in commercial power flow programs as was demonstrated in (TATE AND OVERBYE, 2005), (BRAZ ET AL., 2000) and (GUTIERREZ ET AL., 2011) showing that the representation of voltages in polar coordinates present a better overall performance.

Since it is a nondivergent method, it can overcome convergence problems presented on conventional load flows for ill-conditioned systems, for example. Rather than just diverging, it provides information about the feasible region in case infeasible loading factors are used, which is a very important feature for its application to voltage stability analysis problems. A representation of a particular two parameter (load) space is shown in Figure 2.10 divided into a feasible region like point 1 for which there is an operating point and an infeasible region like point 3 for which operation is not possible (unstable region). Within the feasible region it is assumed that a conventional load flow would converge to an operational point, however, depending on the system's characteristics conventional load flow methods may fail, not converge or even diverge. In the case of a loading point outside of the feasible region (infeasible) the conventional load flow would directly diverge, since in fact there is not a possible operation point. However, it was demonstrated in (OVERBYE, 1994) that results using the LFSSO are those that would be obtained if a loading point on the feasibility boundary (Σ) was taken (point 2), instead of just diverging. Nevertheless, this point is usually in a different loading direction.

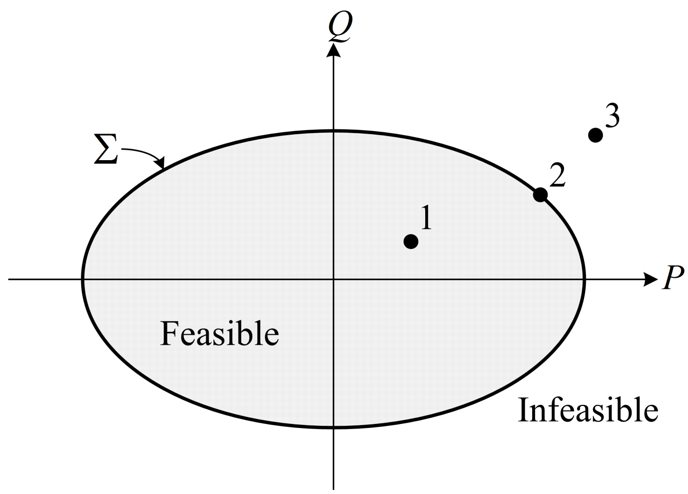

Figure 2.10: Parameter space. Adapted from (DE LIMA TAVARES, 2010)

Another useful characteristic of the LFSSO is that for well-conditioned systems and parameters within the feasible region the optimal multiplier μ takes values close to one, not affecting considerably the conventional method. On the other hand, for systems with no feasible operating point μ tends to assume very low values (theoretically it tends to zero).

A power system can be modeled by the following system of equations, as described in (ARONES, 2010).

$$\mathbf{g}(x,u,p) = 0 \tag{2.11}$$

where **g** are the nodal power mismatches, x the bus voltages including magnitudes and phase angles, u the control variables vector and p the parameters' vector (active and reactive power injections on load buses, active power generation, voltage magnitudes at generator buses, etc.).

At each iteration r, vector Δx is updated as follows.

$$\Delta x^{(r)} = -\left[\nabla_x \mathbf{g}\left(x^{(r)}\right)\right]^{-1} \mathbf{g}\left(x^{(r)}, \rho\right) \quad \text{and} \tag{2.12}$$

$$x^{(r-1)} = x^{(r)} + \mu^{(r)} \Delta x^{(r)} , \tag{2.13}$$

where $\mu^{(r)}$ is the step size (optimization factor) which is multiplied by the correction vector of state variables $\Delta x^{(r)}$ at every iteration r, $\nabla_x \mathbf{g}$ is the Jacobian matrix of $\mathbf{g}$. The multiplier (μ) is calculated in order to minimize the following quadratic function based on the system's power mismatches.

$$\min F(\mu) = \frac{1}{2} \left|\mathbf{g}_{st}\right|^2 = \frac{1}{2} \sum_{i \in \Omega_g} \mathbf{g}_{st,i} , \tag{2.14}$$

with Ω_g as the components of $\mathbf{g}$ taken into account (active and reactive power mismatches at PQ buses and active power mismatches for PV); $\mathbf{g}_{st}$ is $\mathbf{g}$ expanded in Taylor series up to the second order terms, as

$$\begin{aligned} \mathbf{g}_{st}(\mu) &= \mathbf{g}\left(x^{(r)}, \rho\right) + \mu \nabla_x \mathbf{g}\left(x^{(r)}\right) \Delta x^{(r)} + \mu^2 T\left(x^{(r)}\right) \\ \mathbf{g}_{st}(\mu) &= a + \mu\, b + \mu^2\, c\, . \end{aligned} \tag{2.15}$$

$T(x)$ corresponds to the second order derivatives of the power mismatches with respect to the state variables, given by

$$T(x) = \frac{1}{2} \left(\sum_{i \in \Omega_g} \Delta x_i \frac{\partial}{\partial x_i} \right)^2 \mathbf{g}(x) \ . \tag{2.16}$$

By substituting (2.15) in (2.14) and applying the local minimum condition $\frac{\partial F}{\partial \mu} = 0$ as in

(2.17), one gets a cubic equation

$$
\begin{aligned}
\frac{\partial}{\partial \mu}\left(\frac{1}{2}\sum_{i\in\Omega_g}\left(a+\mu\, b+\mu^2\, c\right)^2\right) &= 0\ , \\
g_0+g_1\mu+g_2\mu^2+g_3\mu^3 &= 0\ \text{, where} \\
g_0 &= \sum_{i=1}^{2n}(a_i b_i) \\
g_1 &= \sum_{i=1}^{2n}(b_i^2+2a_i c_i) \\
g_2 &= 3\sum_{i=1}^{2n}(b_i c_i) \\
g_3 &= 2\sum_{i=1}^{2n}(c_i)\ ,
\end{aligned}
\tag{2.17}
$$

that can be solved for μ using direct methods like the Cardano-Tartaglia method or any other method to solve non linear equations, like the Newton-Raphson method.

As it was explained before, for ill-conditioned systems μ assumes optimized values improving the iterative process and giving the right answer by changing the step size; on the other hand for well-conditioned networks it takes values close to the unity, not affecting the original method significantly. Subsequently, for infeasible operation points (due to contingencies or load demand beyond the network's capacity), μ assumes low values, tending to zero $(\mu \to 0)$. When this happens, the solution given by the LFSSO takes values on the feasibility boundary Σ rather than diverging. It should be noticed that the Jacobian matrix is singular for points on Σ, that is why conventional load flows diverge when close to that hypersurface, however, the convergence of the LFSSO is not affected since $\mu^{(r)}\Delta x^{(r)} \to 0$.

3 Determination of the Maximum Loading Point (MLP)

Some basic aspects for the understanding of the voltage stability problem as well as some important tools for its analysis were presented in the previous chapter. In this chapter, two specific methods for voltage stability assessment are described and some tests are carried out, showing their performances to estimate the MLP. The first method is based on phasor measurements and on Thevenin equivalents of the network as seen from the load buses. Two different alternatives of this method are proposed and their results are compared. The second method is an application of the LFSSO for voltage stability analysis. Results using different initial loading values are also shown. Finally, the two alternatives of the first method are named Initializing Methods, since their outputs are used as initial values for the LFSSO based algorithm. Simulation results are also shown.

3.1 Initializing methods

The initializing methods used in this work are based on tracking the Thevenin equivalent of the system as seen from load buses using only local measurements and estimating the MLP based on an impedance matching criterion. This approach has been explored in the literature for several years now, and has shown satisfactory results for both local and wide area monitoring (ZIMA ET AL., 2005), (CORSI AND TARANTO, 2008) and (DAS, 2014), among others. Although they are based on the same principle, the approaches differ on the method they use for finding the critical point. In (VU ET AL., 1999) the load's impedance magnitude is compared with the magnitude of the Thevenin impedance in order to estimate imminent voltage instability. Similarly, in (JULIAN ET AL., 2000) an index was proposed to measure the proximity to voltage collapse also based on Thevenin equivalents but in terms of power rather than impedance using the Voltage Stability Predictor (VIP). In (WARLAND AND HOLEN, 2001) the reach of the VIP was upgraded by adding knowledge from the surrounding area. A voltage based algorithm was proposed in (MILOSEVIC AND BEGOVIC, 2003), where the proposed index relates the reactive power reserves of system's generators and the calculated index to indicate the proximity to voltage collapse. Tellegen's theorem and adjoint networks were also used in (SMON ET AL., 2006) using two sets of measurements to deal with smooth load increases and to calculate the Thevenin parameters and derive a voltage stability index.

The initial idea of the initializing methods proposed in this work is based on the voltage stability margin algorithm of (SU ET AL., 2012). A new measurement-based network-free algorithm was proposed to provide load power margin information based on the impedance matching condition between the load's and Thevenin's impedance magnitudes using PMUs. The estimation of these parameters is done requiring at least two consecutive or close measurements, as explained in the previous chapter.

According to the maximum power transfer theorem, the maximum power that can be delivered to load $\tilde{Z}_i^L$ using the circuit of Figure 2.9 occurs when

$$\left|\tilde{Z}_i^L\right| = \left|\tilde{Z}_i^{th}\right| . \tag{3.1}$$

Figure 3.1 shows the evolution of the load's impedance as the system's loading factor λ increases, finally reaching the MLP when its magnitude matches the magnitude of the Thévenin's impedance.

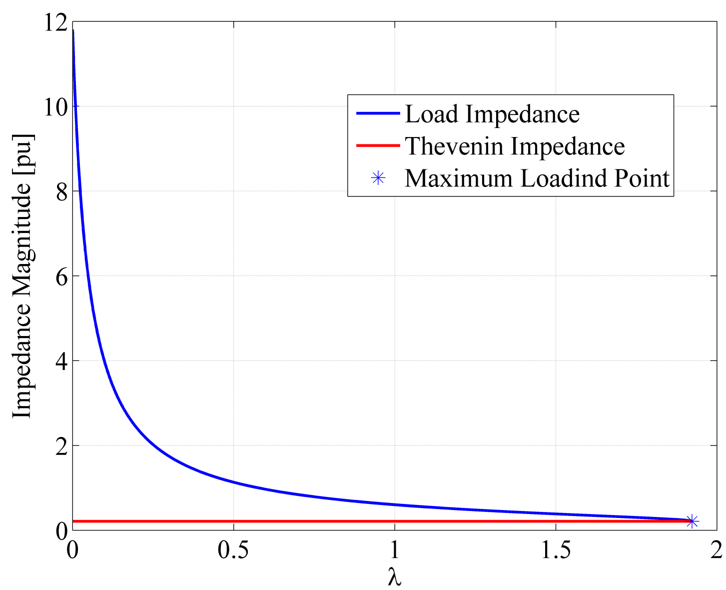

Figure 3.1: Magnitude of load impedance vs Loading factor.

This means that the critical point of the equivalent circuit seen from bus i occurs simultaneously with the load's maximum power consumption. This statement is valid for constant power loads, since depending on the behavior of loads to voltage variations the critical point might change, usually beyond the MLP on the PV curve, as explained in (MILOSEVIC AND BEGOVIC, 2003), showing that the worst case happens when purely constant power loads are modeled. Thus, this is a very interesting point for voltage stability analyses as it easily allows the estimation of the MLP, as shown in Figure 3.1. Besides, it is a conservative point, and adopting it as the power system's actual MLP leads operators to work on the safe side. It should be noted that for small load values (small power consumption) the load impedance assumes higher values. Accordingly, as load increases its impedance decreases and finally at the maximum loading point it assumes the same value as the Thevenin impedance.

The Voltage Stability Margin (VSM), which indicates the percentage of load that can be increased before reaching the critical point, can be obtained by

$$VSM = \frac{P_i^{max}}{P_i} \,, \tag{3.2}$$

where P_i is the current active power at bus i and P_i^{max} is the maximum power transfered to load, i.e. the MLP. The active power P_i is obtained from PMU measurements at bus i, therefore, P_i^{max} becomes the parameter to be estimated. Since the current operation point in most cases is relatively far from the MLP (desired normal operation), the method described in (SU ET AL., 2012) uses load's impedance data for three different operating points and estimates when this value is numerically identical to the calculated Thevenin impedance using an extrapolation technique named Cubic Spline Extrapolation (CSE) (BOOR, 1978). This procedure is made for every load bus in the system.

3.1.1 Maximum loading point using the Cubic Spline Extrapolation

Figure 3.2 shows the process of extrapolation using cubic splines for bus i. The dashed line represents the extrapolation path, $\hat{P}_i^{max}$ is the estimated MLP and $\hat{P}_i^{M}$ the estimated distance between the current operation point and the estimated MLP. It can be seen that there is a difference between the estimated value and the real one, which can be small or large depending on several factors that will be explained later.

Three PMU measurements are needed by the CSE technique. After finding the Thevenin equivalent parameters using two of them, it is possible to extrapolate the value of the impedance

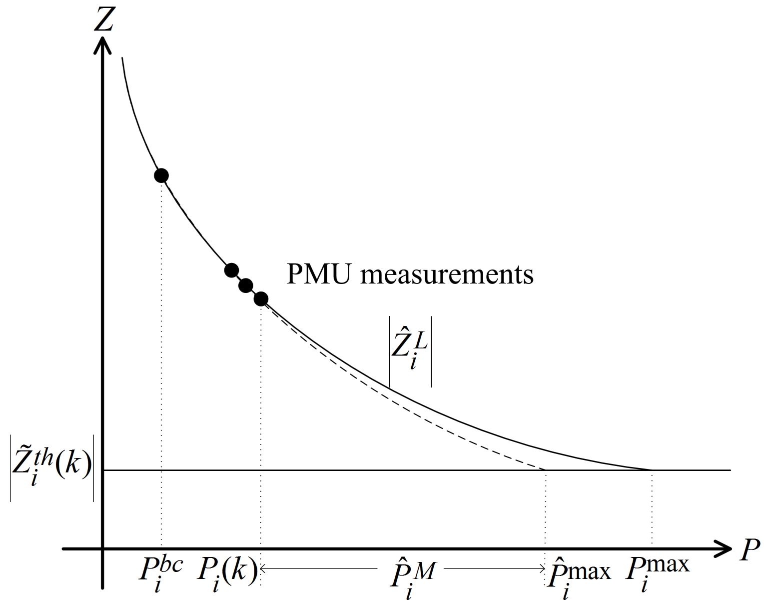

Figure 3.2: Maximum loading point with the CSE based on information from bus i.

magnitude and estimate the corresponding value of active power using cubic splines, that turns out to be the MLP. In order to explain the extrapolation using cubic splines, the interpolation must be understood first. The goal of cubic spline interpolation is to get a function that is smooth on its first derivative, and continuous in the second derivative, both within an interval and at its boundaries (PRESS ET AL., 1992). The function obtained by the spline corresponds to a set of sub-functions, one for each interval.

In a general form, for a set of points $[x_i, y_i]$ with $i = 1, 2, \ldots, m$ and a function $y = f(x)$, the cubic spline function $F(x)$ can be defined as

$$F_j(x) = a_j + b_j\, x_j + c_j\, x_j^2 + d_j\, x_j^3 \qquad j = 1, 2, \ldots, (m-1)\,. \tag{3.3}$$

Since there are $(m-1)$ intervals j and four coefficients for each one (a_j, b_j, c_j, d_j), there are $4(m-1)$ parameters required to completely define $F(x)$. Therefore, in order to find them, an equal number of independent conditions are needed. Following the procedure explained in (BOOR, 1978), for each interval the first two conditions are obtained due to the condition that $F(x)$ be continuous at each point.

$$F_j(x_i) = y_i\,, \qquad i = 1, 2, ..., m\,. \tag{3.4}$$

It is necessary to obtain $2(m-1)$ additional conditions to satisfy the equation system. Then, it is established that the first and second derivatives are continuous for each interval, or

$$F_j^{'}(x_{i+1}) = F_{j+1}^{'}(x_{i+1}) \quad \text{and} \quad F_j^{''}(x_{i+1}) = F_{j+1}^{''}(x_{i+1})\,. \tag{3.5}$$

But those equations only establish $2(m-2)$ conditions, so there are two conditions still missing to solve the equations system. There are different ways to complete the system, nevertheless, the most common, and that will be used in this work is known as "natural solution". It consists of making the second derivatives of the first and the last point of the data set equal to zero, leading to a simple linear system which can be solved easily to provide the coefficients of the polynomials. These equations are

$$F_1^{''}(x_1) = 0 \quad \text{and} \quad F_{m-1}^{''}(x_m) = 0\,. \tag{3.6}$$

As explained earlier, only three PMU measurements relating active power (x_k) and the magnitude of load's impedance (y_k) are needed to estimate the MLP, hence, in this case $m = 3$, leading to a system of eight variables and the same number of equations relating the three points and two intervals as follows.

$$[x_k, y_k] = \left[\left|\tilde{Z}_i^L(k)\right|, P_i(k)\right]\,, \qquad k = 1, 2, 3 \tag{3.7}$$

$$
\begin{bmatrix}
1 & x_1 & {x_1}^2 & {x_1}^3 & 0 & 0 & 0 & 0 \\
1 & x_2 & {x_2}^2 & {x_2}^3 & 0 & 0 & 0 & 0 \\
0 & 1 & 2x_2 & 3{x_2}^2 & 0 & -1 & -2x_2 & -3{x_2}^2 \\
0 & 0 & 2 & 6x_2 & 0 & 0 & -2 & -6x_2 \\
0 & 0 & 0 & 0 & 1 & x_2 & {x_2}^2 & {x_2}^3 \\
0 & 0 & 0 & 0 & 1 & x_3 & {x_3}^2 & {x_3}^3 \\
0 & 0 & 2 & 6x_1 & 0 & 0 & 0 & 0 \\
0 & 0 & 0 & 0 & 0 & 0 & 2 & 6x_3
\end{bmatrix}
\begin{bmatrix} a_1 \\ b_1 \\ c_1 \\ d_1 \\ a_2 \\ b_2 \\ c_2 \\ d_2 \end{bmatrix}
=
\begin{bmatrix} y_1 \\ y_2 \\ 0 \\ 0 \\ y_2 \\ y_3 \\ 0 \\ 0 \end{bmatrix}
\tag{3.8}
$$

However, this procedure only allows finding the functions between the three measured points for both intervals (interpolation). After solving the equation system and finding all coefficients it is possible to extrapolate and estimate the value of the active power at the MLP by substituting the Thevenin's impedance magnitude value $\left|\tilde{Z}_i^{th}(k)\right|$ into the function of the last interval $(F_2(x))$. This procedure is carried out for all load buses.

Finally, the method in (SU ET AL., 2012) proposes a VSM using (3.9) and (3.10), where $P_i(k)$ is the measured active power at bus i, n is the number of load buses and $\hat{P}_i^{max}$ is the maximum power estimated at that bus using the CSE.

$$
\hat{P}_i^M = \hat{P}_i^{max} - P_i(k)\,, \qquad i = 1, 2, ..., n \tag{3.9}
$$

$$
\text{VSM}_0 = \frac{\sum_{i=1}^{n} \hat{P}_i^M}{\sum_{i=1}^{n} P_i(k)} + 1 = \frac{\sum_{i=1}^{n} \hat{P}_i^{max}}{\sum_{i=1}^{n} P_i(k)} \tag{3.10}
$$

3.1.2 Proposed initializing method 1

As shown before, the VSM used in (SU ET AL., 2012) takes into account the information from all load buses; however, it is expected that when both load and generation are uniformly scaled, the voltage collapse occurs at the weakest bus first, this is, the bus that defines the MLP.

This bus can be found based on the fact that the VSM of all load buses can be estimated using the original method (SU ET AL., 2012) and that it is possible to identify the weakest bus in the system by just comparing their particular proximity to the critical point (HAQUE, 2003). In other words, the *Initializing method 1* takes into account one bus only, namely the weakest one i, determined by

$$\hat{P}_i^M = \min\left\{\hat{P}_j^{max} - P_j(k)\right\}\,, \qquad j = 1, 2, ..., n\,, \tag{3.11}$$

where n is the number of monitored buses. Once the weakest bus i is known, it is possible to analytically estimate the MLP by

$$\begin{aligned} &V_i^4 + V_i^2\left[2\left(r_i^{th}\hat{P}_i^{max} + x_i^{th}\hat{Q}_i^{max}\right) - \left(\hat{E}_i^{th}\right)^2\right] + \\ &+ \left(r_i^{th}\hat{Q}_i^{max} - x_i^{th}\hat{P}_i^{max}\right)^2 + \left(r_i^{th}\hat{P}_i^{max} - x_i^{th}\hat{Q}_i^{max}\right)^2 = 0\,. \end{aligned} \tag{3.12}$$

Eq. (3.12) is adapted from Eq. (2.4) for the Thevenin equivalent as seen from the weakest bus, and can be written as $aV_i^4 + bV_i^2 + c = 0$. Making the discriminant equal to zero, $b^2 - 4ac = 0$, case when both roots are real and identical (bifurcation point), and assuming constant power factor it is possible to determine the MLP ($\hat{P}_i^{max}$) knowing that $\hat{Q}_i^{max} = \hat{P}_i^{max}\left(\frac{Q_i(k)}{P_i(k)}\right)$. Finally, the system's VSM can be calculated as

$$\mathrm{VSM}_1 = \frac{\hat{P}_i^{max}}{P_i(k)} \tag{3.13}$$

3.1.3 Proposed initializing method 2

The proposed initializing method 2 is based on the idea of the Pareto's principle, originally proposed as an economic law describing income (PARETO, 1964), but that has been widely used in many other areas as explained in (PINTO ET AL., 2012).It basically states that the relative number of individuals with an annual income larger than a certain value x was proportional to a power of x. Since voltage stability is described as a local phenomena affected by just a portion of the system buses, the initializing method 2 proposes the use of the Pareto's principle to obtain a set of critical buses. Using the estimated TE of every monitored bus i, considering $P_i(k)$ and solving (3.12) for all of them, the MLP of each equivalent circuit can be computed without using the CSE. Then, the most representative load buses are identified, rather than using one single bus only to compute stability margin. The idea is to determine a certain number of buses that represent the behavior of the network, so additionally to the procedure of finding the MLP using the analytic equation, the identification of the most representative buses must also be carried out. Initially, the following quantities are computed for each load bus.

$$\begin{aligned} a_i &= 1 - \frac{\hat{P}_i^{max} - P_i(k)}{\hat{P}_i^{max}} = \frac{P_i(k)}{\hat{P}_i^{max}}\text{, and} \\ w_i &= \frac{a_i}{\sum_{l=1}^{n} a_z}\text{, for } i = 1, 2, ..., n\,. \end{aligned} \tag{3.14}$$

The load buses are sorted in descending order of w_i and stored in **W**. Then, a vector **S** containing the cumulative sum of the elements of **W** is calculated and each of its elements compared with a threshold value γ. The first element grater than the threshold, j, defines which buses must be taken into account in the calculation of the VSM, resulting in a group of representative buses $(1, 2, ..., j)$ as shown in (3.15). Note in (3.14) that this is valid only for $P_i(k) \leq \hat{P}_i^{max}$, so the sum of all w_i is equal to the unity.

$$\begin{aligned} \mathbf{W} &= \{w_1, w_2, ..., w_n \mid w_1 > w_2 > ... > w_n\} \\ \mathbf{S} &= \left\{ \sum_{i=1}^{k} w_i \mid k = \{1, 2, ..., n\} \right\} \\ \text{where} \quad s_1 &= w_1 \quad \text{and} \quad s_n = 1 \quad \text{and } s_k \in \mathbf{S} \\ s_j &= \{\min(\mathbf{S}) \mid s_k \geq \gamma\} \end{aligned} \tag{3.15}$$

Finally, the calculation of the VSM must be performed only for those selected buses as

$$\text{VSM}_2 = \frac{1}{j}\sum_{i=1}^{j}\frac{\hat{P}_i^{max}}{P_i(k)} \tag{3.16}$$

where the summation includes the first j buses for which $\sum_{i=1}^{j} w_i \geq \gamma$. Note that while the *Initializing method 1* takes only one bus to compute the initial value of ρ, the second one takes a certain number of buses that represent the behavior of the network. This difference is shown later on this chapter.

3.1.4 Example using initializing methods

A simple 3-bus system will be used as an example. The system's bus data for the base case are shown in Table 3.1, branch data in Table 3.2 and the one-line diagram in Figure 3.3. The actual MLP of this system is $P^{max} = 7.87$ p.u or a VSM $= 1.10$, this is, the system has a 10% margin before reaching the MLP. The aim of the example is to estimate the Thevenin equivalent parameters, the MLP and the VSM using the initializing methods explained before. Three different operation points obtained using a conventional load flow algorithm were used to simulate the three PMU voltage and current measurements.

Table 3.1: System bus data

Bus	**Type**	$\mathbf{V}_g$	$\mathbf{P}_g^{bc}$	$\mathbf{Q}_g^{min}$	$\mathbf{Q}_g^{max}$	$\mathbf{P}_{bc}$	$\mathbf{Q}_{bc}$
1	Slack	1.00	-	-	-	-	-
2	PQ	-	-	-	-	3.5	1.5
3	PV	0.98	1	-0.15	0.3	0	0

Table 3.2: System branch data

From	**To**	**R**	**X**	**B**
1	2	0.0100	0.0500	0
2	3	0.0200	0.0600	0
1	3	0.0125	0.0400	0

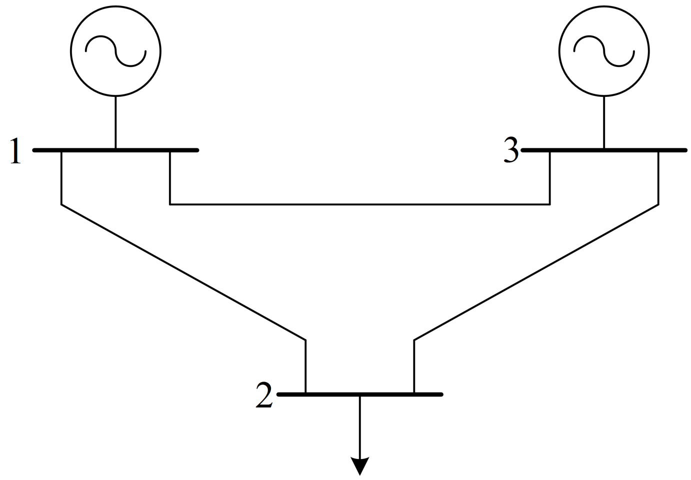

Figure 3.3: 3-bus system one-line diagram.

- **Load flow results (PMU measurements)** As explained before, the results from a conventional load flow for three different operational points are used. These results are shown in Table 3.3, where the sample number is defined as k, the loading factor, multiplying the base case as λ, bus voltage magnitude and phase angle as $\mathbf{V}$ and $\boldsymbol{\theta_V}$ respectively. Similarly for bus current and finally for load impedance using $\mathbf{I}$, $\boldsymbol{\theta_I}$, $\mathbf{Z}_L$ and $\boldsymbol{\theta_{ZL}}$.

Table 3.3: Results for bus 2 after running conventional load flows.

Sample (k)	$\boldsymbol{\lambda}$	**V**	$\boldsymbol{\theta_V}$ (°)	**I**	$\boldsymbol{\theta_I}$ (°)	$\boldsymbol{Z_L}$	$\boldsymbol{\theta_{Z_L}}$ (°)
1	2	0.7214	-14.9316	10.5568	-38.1302	0.0683	23.1986
2	2.02	0.7151	-15.2321	10.7567	-38.4306	0.0665	23.1986
3	2.04	0.7085	-15.5461	10.9648	-38.7447	0.0646	23.1986

- **Thevenin equivalent parameters estimation**

  The estimation of Thevenin's parameters is done following the procedure explained in Chapter 2. Since there is only one load bus, it is only necessary to estimate one equivalent circuit using (2.8) with the values of the two most recent measurements shown in Table 3.3 using $k = 3$, leading to

$$\begin{bmatrix} 1 & -\tilde{I}_i(k) \\ 1 & -\tilde{I}_i(k-1) \end{bmatrix} \begin{bmatrix} \tilde{E}_i^{th} \\ \tilde{Z}_i^{th} \end{bmatrix} = \begin{bmatrix} \tilde{V}_i(k) \\ \tilde{V}_i(k-1) \end{bmatrix}$$

$$\begin{bmatrix} 1 & -(10.9648\angle-38.74) \\ 1 & -(10.7567\angle-38.43) \end{bmatrix} \begin{bmatrix} \tilde{E}_2^{th} \\ \tilde{Z}_2^{th} \end{bmatrix} = \begin{bmatrix} 0.7085\angle-15.55 \\ 0.7151\angle-15.23 \end{bmatrix}$$

$$\begin{bmatrix} \tilde{E}_2^{th} \\ \tilde{Z}_2^{th} \end{bmatrix} = \begin{bmatrix} 1.0165\angle 0.7301 \\ 0.0356\angle 70.0257 \end{bmatrix} = \begin{bmatrix} 1.0164 + j0.0130 \\ 0.0122 + j0.0335 \end{bmatrix}$$

- **Maximum loading point using Cubic Spline Extrapolation**

  The CSE technique is used to estimate the point where the magnitude of load's impedance matches numerically with the magnitude of Thevenin's impedance. Following the procedure explained before in this chapter, the matrix of data for the example system is

$$\begin{bmatrix} x_1 & y_1 \\ x_2 & y_2 \\ x_3 & y_3 \end{bmatrix} = \begin{bmatrix} \left|\tilde{Z}_2^L(1)\right| & P_2(1) \\ \left|\tilde{Z}_2^L(2)\right| & P_2(2) \\ \left|\tilde{Z}_2^L(3)\right| & P_2(3) \end{bmatrix}$$

  It should be noticed that both, base case load and generation were scaled by loading factor λ. The next step is to solve the system of equations to find the spline coefficients, leading to the following equation for both intervals.

$$F_{1,2}(x) = -553.1848\, x^2 + 35.6804\, x + 7.1436$$

  Coincidently, the coefficients of both quadratic functions are approximately equal. Finally, it is possible to extrapolate and find the MLP using the function of the latest interval $(F_2(x))$.

$$F_2\left(\left|Z_2^{th}\right|\right) = \hat{P}_2^{max} = 7.7127$$

$$\hat{P}_2^{M} = \hat{P}_2^{max} - P_2(3) = 7.7127 - 7.14 = 0.5726$$

  Since there is only one load bus, one gets

$$VSM_0 = \frac{\sum_{i=1}^{n} \hat{P}_i^M}{\sum_{i=1}^{n} P_i(k)} + 1 = \frac{0.5726}{7.14} + 1 = 1.0802$$

  Meaning that the current load can be increased in 8.02% before reaching the MLP.

- **Maximum loading point using the proposed method 1**

Since the method uses the MLP obtained using the CSE technique to calculate the weakest bus, the information of the previous example can be used again. However, there is only one load bus, meaning that it is the closest to the critical point

$$\hat{P}_i^M = \min\left\{\hat{P}_i^{max} - P_j(k)\right\} = \hat{P}_2^M = 0.5726$$

This means that $i = 2$ is the weakest bus, thus (3.12) can be rewritten as

$$a = 1$$
$$b = 2\left(r_2^{th}\hat{P}_2^{max} + x_2^{th}\hat{Q}_2^{max}\right) - \left(\tilde{E}_2^{th}\right)^2$$
$$c = \left(r_2^{th}\hat{Q}_2^{max} + x_2^{th}\hat{P}_2^{max}\right)^2 + \left(r_2^{th}\hat{P}_2^{max} + x_2^{th}\hat{Q}_2^{max}\right)^2$$

The values of the Thevenin equivalent are known. Writing the equation in terms of $\hat{P}_2^{max}$ one gets

$$\hat{Q}_2^{max} = \hat{P}_2^{max}\left(\frac{Q_2(3)}{P_2(3)}\right) = \hat{P}_2^{max}\left(\frac{3.06}{7.14}\right)$$

Finally, $\hat{P}_i^{max}$ is found by

$$b^2 - 4ac = 0$$
$$\hat{P}_i^{max} = \begin{cases} 9.4087 \longleftarrow \text{ (most reasonable value)} \\ -287.5852 \end{cases}$$
$$VSM_1 = \frac{\hat{P}_2^{max}}{P_2(3)} = \frac{9.4087}{7.14} = 1.3177$$

Which means that the current load can be increased in 31.77% before reaching the MLP.

- **Maximum loading point using the proposed method 2**

The second method does not use the CSE technique to find the MLP, instead, it must be calculated analytically using Eq. 3.12 and the Thevenin equivalent for all load buses. Since this system only has one load bus, it means that it automatically turns into the weakest bus; then an almost identical procedure to the one used for method 1 is again applied for this particular test system. However the method for choosing the weakest bus is a little bit different, assuming a value of $\gamma = 0.8$, the procedure is

$$a_2 = 1 - \frac{9.4087 - 7.14}{9.4087} = \frac{7.14}{9.4087} = 0.7589$$

$$w_2 = \frac{0.7589}{\sum_{l=1}^{n} a_l} = 1$$

$$\mathbf{W} = \{w_1, w_2, ..., w_n \mid w_1 > w_2 > ... > w_n\} = \{1\}$$

$$\mathbf{S} = \left\{ \sum_{i=1}^{k} w_i \mid k = \{2\} \right\}$$

$$s_j = \{\min(\mathbf{S}) \mid s_k \geq \gamma\} \rightarrow s_j = s_2$$

So, it was inferred that the weakest bus is number two. Even though the result is intuitive, it must be shown since this is the main difference between *Initializing method 1* and *Initializing method 2* when there is more than one load bus.

It could be seen that the method that better estimates the MLP for this particular example system is the original method proposed in (SU ET AL., 2012). A VSM of approximately 1.08% was estimated, which means that the load can increase up to 8% from the actual operating point ($\rho = 2.04$) before the system reaches the MLP. The reference value for the VSM at that operating point is 10% using successive load flows as estated at the beginning of the example, which means that the estimation was pretty approximated. The obtained results were not that good using the other proposed initializing methods, with significantly higher errors (19%). Nevertheless, this kind of result is not frequent, as it will be conclude later on this work. Finally the flowchart of the general method is presented in Figure 3.4.

3.2 Performance of Initializing Methods

Two basic tests were carried out to compare the proposed initializing methods and the method in (SU ET AL., 2012) using the IEEE test systems with 14, 30, 57 and 118 buses. It was also tested a realistic portion of the Brazilian transmission system (year 2010) with a total of $4{,}526$ buses, 500 generation buses with 65.191 GW of total generation, and a base load of 65.078 GW and

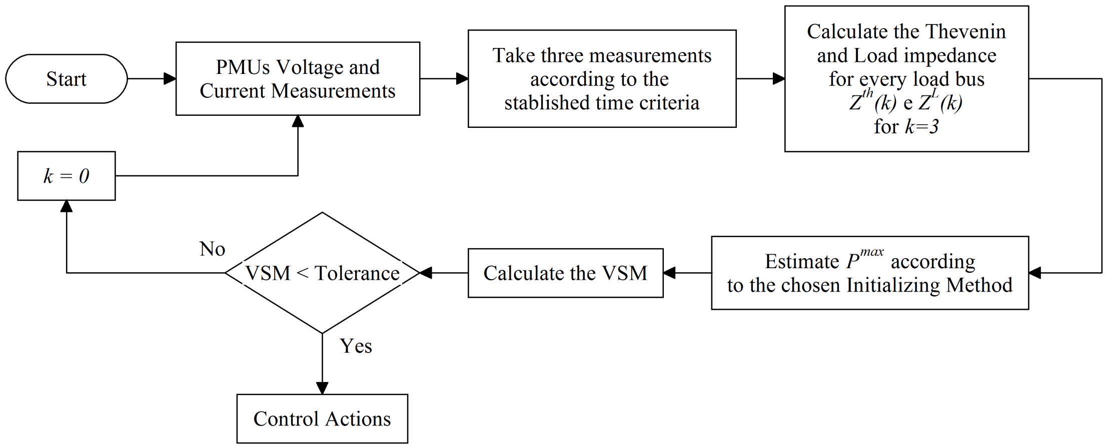

Figure 3.4: Flowchart of the general method.

21.494 GVAr. In the first test case all generators and loads were modified by the same scale factor (λ), in order to simulate a daily load curve, deliberately driving each system relatively near to its MLP. Also, the interval between samples was equally spaced in terms of active power variation. The second test case was set up to simulate a more realistic scenario, so the values of λ took different random values around the daily load curve mentioned earlier for all buses. An example of these values for a particular test system is shown in Figure 3.5, where a slight difference can be seen between the red line, relating the loading factors for all load buses used in the first test and the blue one with the respective values of one particular bus for the second.

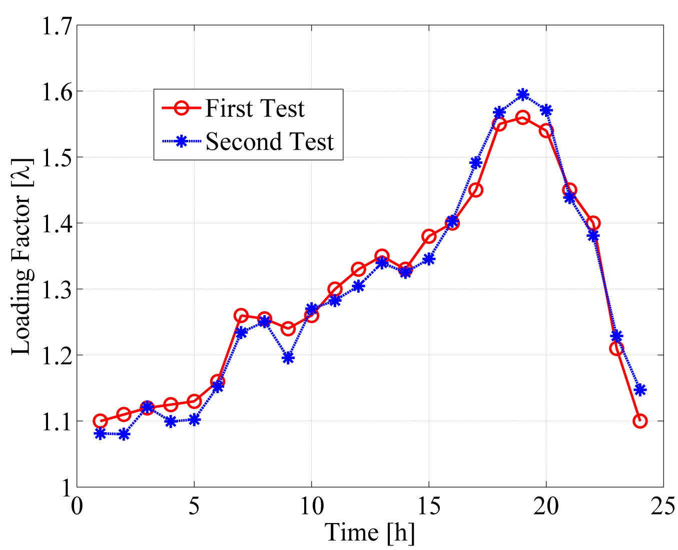

Figure 3.5: Daily load curve -– IEEE 14-bus test system.

It clearly shows a slight difference between the first and the second test. Moreover, the second test also takes into account differences between the steps, or time criteria, of each PMU sample as shown in Figure 3.6.

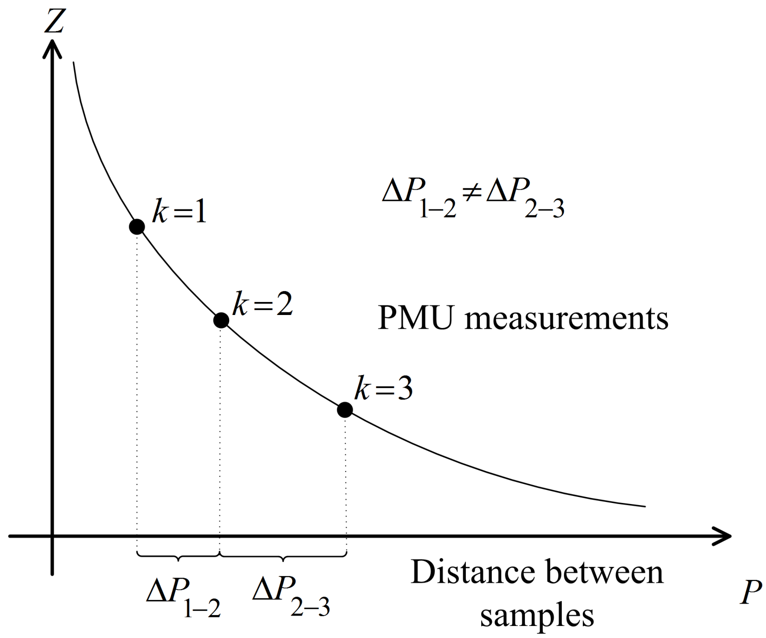

Figure 3.6: Interval between phasor measured samples for the second test.

Finally, the VSMs obtained using the proposed initializing methods and the one in (SU ET AL., 2012), hereafter named *BMethod*, were compared with the margin computed by running successive power flows, progressively increasing the loading factor in loads and generators until they did not converge. This was made for every hour period and is referred to as the Reference Method (*ref*). The figures presented ahead relate the VSM and changes in load for a twenty four hour period in intervals of one hour. For comparison purposes, the relative mean error and the error's standard deviation during the day are defined as

$$\varepsilon_h = \frac{VSM_{ref,h} - VSM_{m,h}}{VSM_{ref,h}} \cdot 100\% \,, \tag{3.17}$$

$$\mu_m = \frac{1}{24} \sum_{h=1}^{24} \mid \varepsilon_h \mid \text{ and} \tag{3.18}$$

$$\sigma_m = \sqrt{\frac{1}{24} \sum_{h=1}^{24} (\mid \varepsilon_h \mid - \mu_m)^2} \,. \tag{3.19}$$

where m is the considered method (*Initializing method 1*, *Initializing method 2* or *BMethod*), h is the hour under test and ref is the reference method.

3.2.1 First test

In the first scenario all generators and loads were scaled with the same value of λ. The time criteria or time between samples was simulated as a difference in terms of loading factor and was fixed at 0.01 p.u. (ΔP_{m-n}). The value of γ was set to 0.5. Generator's reactive power limits were enforced. The VSM and the relative error for the IEEE 14-bus test system are shown in Figure 3.7. VSM using the two proposed initializing methods as well as the *BMethod* are plotted together with the reference values for a period of 24 hours. Also, the relative error between each method and the reference method is also plotted.

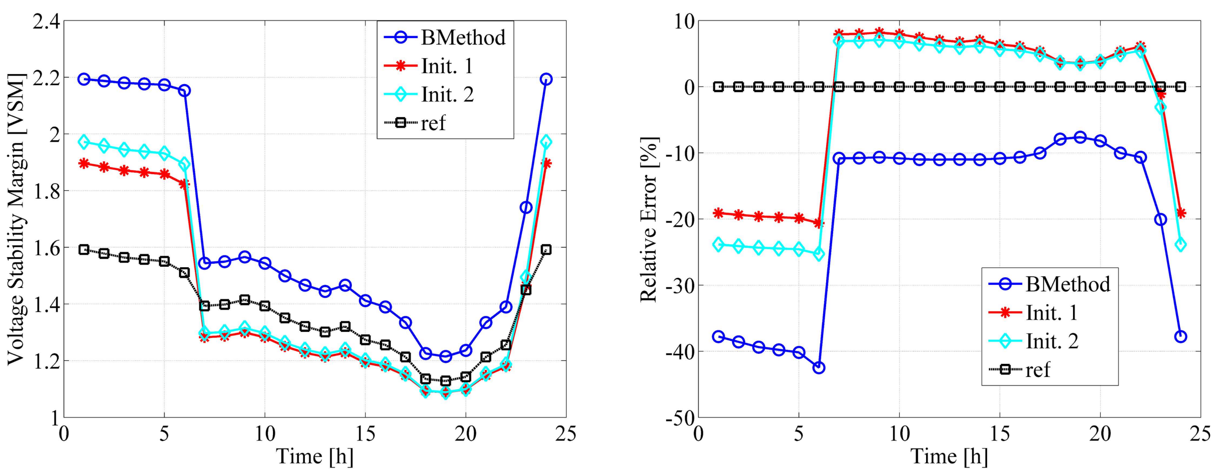

Figure 3.7: Voltage stability margin and relative error – IEEE 14-bus test system, first test.

From Figure 3.7 and Figure 3.8 it can be noticed that all three methods have overall good performance, namely, when load increases the VSM decreases and vice versa. Even though they have a good behavior, it is clear that all of them show larger errors under light load, such as in the early morning period. This basically happens because of the distance between the actual operation point and the critical point, since depending on the system's characteristics, whenever the operating point approaches the critical point the behavior of load impedance with respect to active power is to become more non linear, as can be inferred from Figure 3.1, facilitating the estimation of the MLP using the extrapolation procedure. This is valid specifically in the case of the *BMethod* and the *Initializing method 1*, since they use the CSE to estimate as part of their algorithm. Another reason, that relates both previously mentioned methods and also includes the *Initializing method 2* is basically the estimation of the Thevenin equivalent, since some nonlinearities like generators reaching their reactive power limit between samples or significant variations in the topology of the network can cause errors in the final estimation.

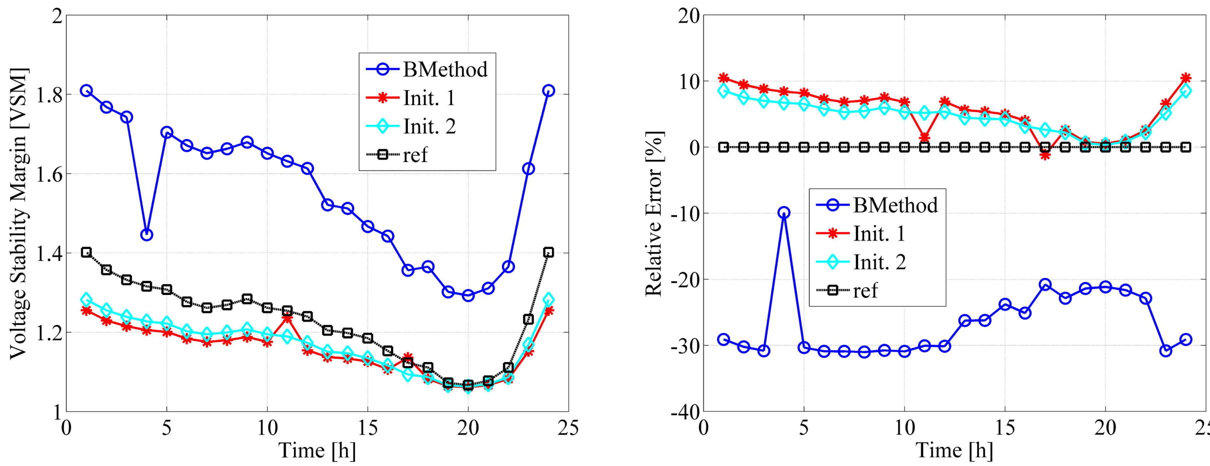

Figure 3.8: Voltage stability margin and relative error – IEEE 118-bus test system, first test.

The absolute mean errors and their respective standard deviations for all tested systems are shown in Table 3.4.

Table 3.4: Absolute mean error and standard deviation – First test.

Test System	μ_{BM}	σ_{BM}	$\mu_{Init.1}$	$\sigma_{Init.1}$	$\mu_{Init.2}$	$\sigma_{Init.2}$
14-bus	17.30	13.20	9.97	6.55	11.56	13.50
30-bus	19.70	18.94	5.36	7.02	6.49	6.88
57-bus	62.99	38.42	4.94	2.67	8.75	1.85
118-bus	25.20	3.45	4.42	2.63	2.50	1.43
4,526-bus	3.62	0.14	2.18	1.23	2.49	0.50

Another advantage of using either of the proposed initializing methods is that they also allow the determination of the weakest bus or buses in the network, depending on the method used. As explained before in this chapter, the *Initializing method 1* selects the bus that has been estimated to the closest to the MLP, i.e. the weakest bus. On the other hand, the *Initializing method 2* uses an algorithm to choose several buses, generally more than one, that were cataloged as the more critical. As an example of this, the chosen buses using each of the proposed initializing methods for a period of 24 hours for the IEEE test systems of 30 and 118 buses are shown in Figure 3.9 a) and b)

respectively. This figure was made by counting the times (frequency) each bus was selected along the 24 hour period. For example, in a) bus 15 was chosen as one of the weakest buses in 15 out of the 24 periods using the *Initializing method 2*. However, it was not chosen in any period when using the *Initializing method 1* since bus 30 was the weakest bus for all tested periods. Similarly, in b) bus 40 was found to be the weakest bus in 9 out of the 24 periods, whereas bus 41 was the chosen one for the remaining 15 periods using the *Initializing method 1*. As for *Initializing method 2*, bus 20, for instance, was selected in all 24 periods and the same happened with other buses, as 42, 43, and so on.

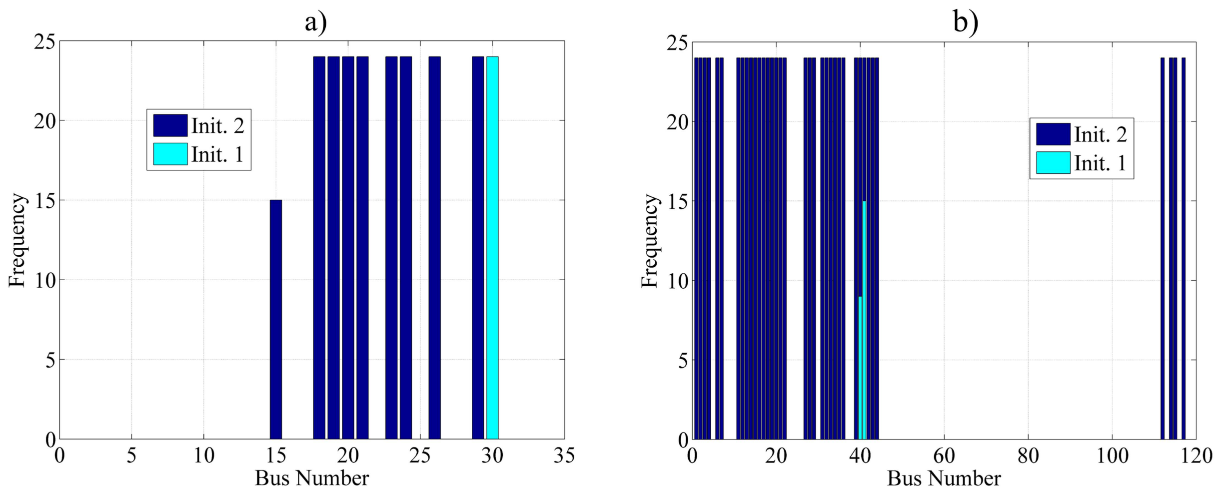

Figure 3.9: Critical buses – IEEE 30-bus and IEEE 118-bus test systems, first test.

The relationship between the number of load buses and the buses used at least once in the 24 periods for the calculation of the MLP is shown in Table 3.5. It can be seen that the number of buses used is considerably reduced in the proposed initializing methods when compared with the *BMethod*. As expected, the number of buses used by the *Initializing method 1* is noticeably smaller than of those used by the *Initializing method 2*.

3.2.2 Second test

In the second case λ took random values around the loading factors used in the first test, with a coefficient of variation $CV = 2\%$ taking the factors used on the first test as mean values. As in the first case, the value of γ was set at 0.5 and, as explained before, the time criterion was no longer controlled since the samples were random values, also with a $CV = 2\%$. As in the first test, the

Table 3.5: Used buses according to the initializing method – First test.

Test System	Load Buses	Used Buses		%	
		Init. 1	Init. 2	Init. 1	Init. 2
14-bus	11	1	5	9.09	45.45
30-bus	21	1	10	4.76	47.62
57-bus	42	1	16	2.38	38.10
118-bus	91	2	37	2.20	40.66
4,526-bus	1978	1	945	0.05	47.78

VSM and the relative error using each method were plotted in Figure 3.10, this time for the IEEE 57–bus test system. As it can be seen, the results obtained with the *BMethod* present larger errors than the ones obtained with the proposed initializing methods.

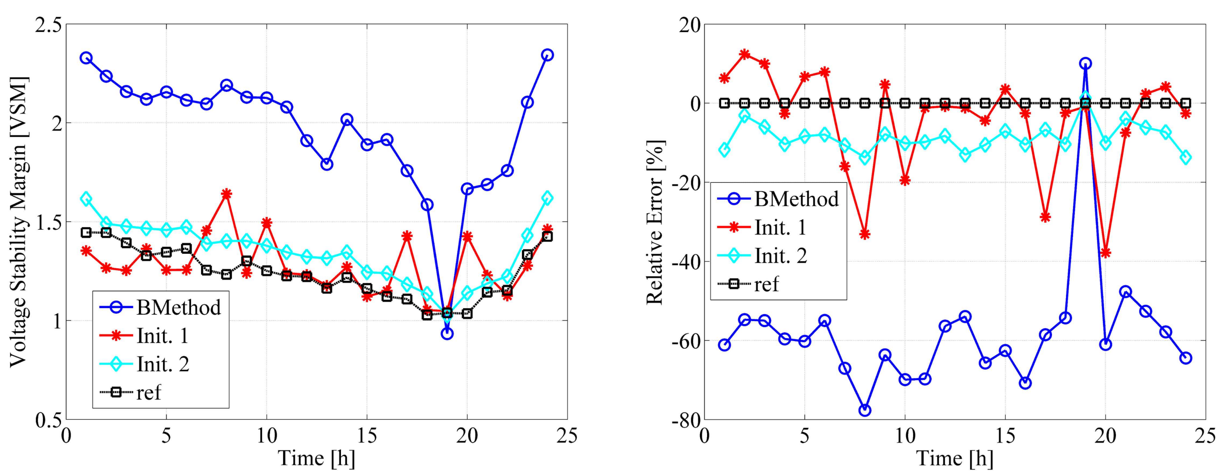

Figure 3.10: Voltage stability margin and relative error – IEEE 57-bus test system, second test.

A similar behavior can also be seen in Figure 3.11 for the Brazilian transmission system where the *Initializing method 1* seems to be more erratic on its estimations since it only takes the value of a single bus to estimate the MLP and variations on this bus affect directly the final result. It provides good estimations but its values constantly change, sometimes leading to higher errors. The *Initializing method 2*, on the other hand, is more robust and in some periods more accurate than the other methods since it is based in more than one bus. Table 3.6 shows the absolute mean errors and its standard deviations using the initializing methods.

The number of critical buses behave similarly in both tests for the *Initializing method 2*. The

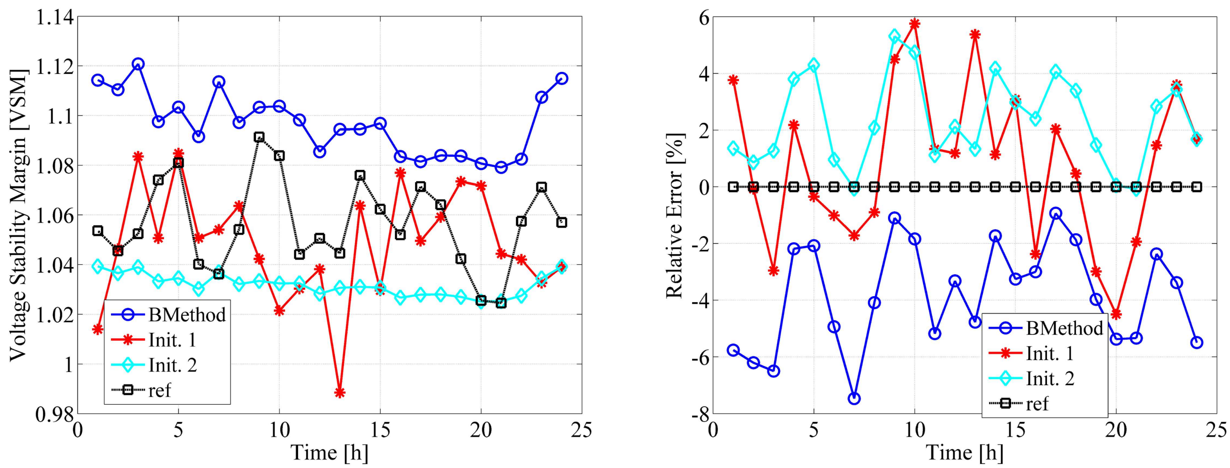

Figure 3.11: Voltage stability margin and relative error – Brazilian 4,526-bus system, second test.

Table 3.6: Absolute mean error and standard deviation – Second test.

Test System	μ_{BM}	σ_{BM}	$\mu_{Init.1}$	$\sigma_{Init.1}$	$\mu_{Init.2}$	$\sigma_{Init.2}$
14-bus	31.10	5.16	18.23	1.49	9.74	1.12
30-bus	25.34	4.70	15.76	0.93	5.38	0.72
57-bus	57.30	15.71	9.14	13.09	8.69	3.41
118-bus	20.38	5.02	10.86	2.67	4.49	1.12
4,526-bus	3.84	1.81	2.35	1.54	2.33	1.52

only difference occurs for the Brazilian system, and it is just of two buses. For all other systems the number of used buses does not change at all as shown in Table 3.7. On the other hand, for *Initializing method 1* the number of used buses during the 24 periods increase significantly as compared with the first test. The critical buses determined for the IEEE 57-bus test system and for the Brazilian transmission system are shown in Figure 3.12. In the case of the Brazilian system, the four buses indicated as the most critical over the tested period using the *Initializing method 1* were bus 3,637 in 16 periods, bus 3,638 in four and finally buses 3,871 and 3,889 in two.

Table 3.7: Used buses according to the initializing method – Second test.

Test System	Load Buses	Used Buses		%	
		Init. 1	Init. 2	Init. 1	Init. 2
14-bus	11	3	5	27.27	45.45
30-bus	21	4	10	19.05	47.62
57-bus	42	4	16	9.52	38.10
118-bus	91	10	37	10.99	40.66
4,526-bus	1978	4	943	0.20	47.67

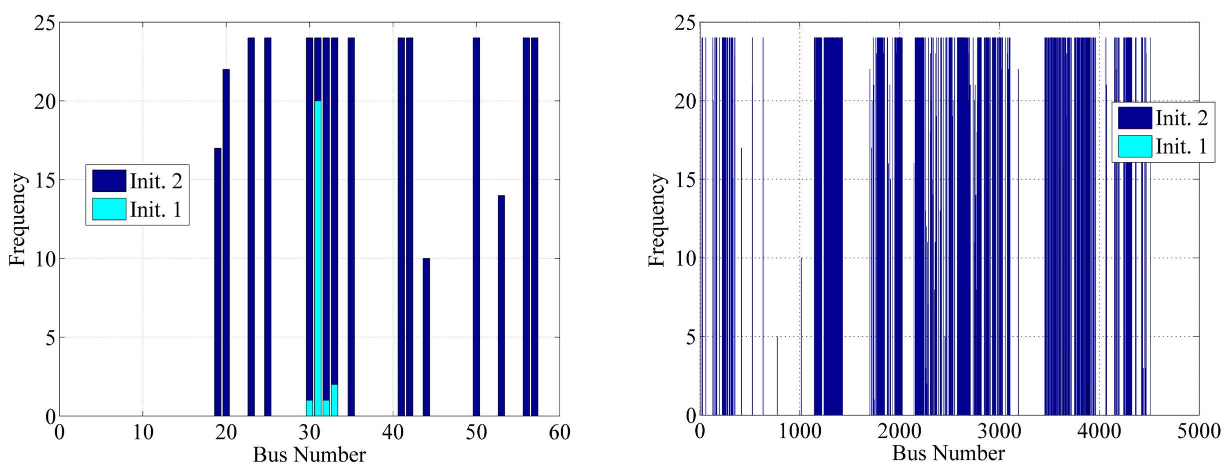

Figure 3.12: Critical buses -– IEEE 57-bus test system and Brazilian 4,526-bus, second test.

Several conclusions can be made from the two performed testes. The first and more important conclusion is that both proposed methods have considerably better performance that the *BMethod* in terms of accuracy. Based on the results obtained it can be said that the *BMethod* has a good performance in some tested systems, particularly when load approaches the critical point since the CSE is more accurate when the operation point is closer to the MLP. Nevertheless, it is also expected that the initializing method behaves satisfactorily most of the time, for different loading factors and be independent to variations in the time criteria since it will be used as a previous step of a more robust method. In this case the use of one of the proposed initializing methods is suggested since they behave considerably better than the *BMethod* to estimate the VSM and the MLP keeping its simplicity and low computational burden. Moreover, the proposed initializing methods need considerably less information since the calculation of the MLP is made using only a portion of the load buses rather than using all load buses. The *Initializing method 1* was the more accurate method in the first test, notwithstanding, for the second test it presented considerably higher mean errors than *Initializing method 2*. This happened because when loading factors and time criteria took random values, as in the second test, the estimation based on the weakest bus in *Initializing method 1* can be affected by the extrapolation process; also, taking only one bus to calculate the MLP makes it more sensitive to estimation errors. The last conclusion is that both proposed initializing methods are able to calculate the system's critical bus; however, *Initializing method 2* also provides a set of additional buses that are also critical. In fact, it could be seen that the critical bus found with *Initializing method 1* was always present within the set of buses established by the *Initializing method 2*.

3.3 Load Flow with Step Size Optimization for Voltage Stability Analysis

There are some methods using the LFSSO for voltage stability assessment in the literature, all of them based on a propriety of the optimal multiplier (μ) when an excessive loading factor ($\rho^0 > \rho^{mlp}$) is used in the LFSSO. Under this circumstances, it was shown in (OVERBYE, 1994) that the method converges to a point on the feasibility border Σ when $\mu \to 0$. Using the additional information provided by the optimal multiplier, a method to calculate the MLP in a predefined load increase direction is proposed in (BEDRIÑANA AND CASTRO, 2008). Since the feasibility boundary contour in the neighborhood of the MLP may be nonconvex, some of the computed approximations may fall within the feasible region, thus, a mechanism based on binary search was used to drive the operating point back to the infeasible region, where the method behaves satisfactorily. However this binary search was really time consuming and the original method does not admit initializing values in the feasible zone. These drawbacks were overtaken later in (TAVARES ET AL., 2010) presenting a method that admits feasible initializing loading factors and a more efficient algorithm to respond to operation points in the feasible zone; it also proposed an error margin that can be provided by the system operator for real applications. Finally (XAVIER ET AL., 2013) uses the best of both previous methods and also includes the analysis of load variation by areas and improves the original algorithm to obtain a better performance when applied to transmission and distribution systems. There are other methods like (LI ET AL., 2010) that also use the LFSSO to estimate the MLP using a predictor–corrector framework for its fast estimation using a common scaling factor but does not consider generators reactive limits.

In fact, the method that will be shown here is the one used in (XAVIER ET AL., 2013) that uses the advantages of the original method and its upgrades, using as stop criteria a previously defined permissible margin of error ($\pm x\%$).

3.3.1 Load Shedding Technique

Assuming an initial point in the infeasible region ($\rho^0 \geq \rho^{mlp}$), the LFSSO converges to the point MLP^0 on the feasibility boundary, as shown in Figure 3.13.

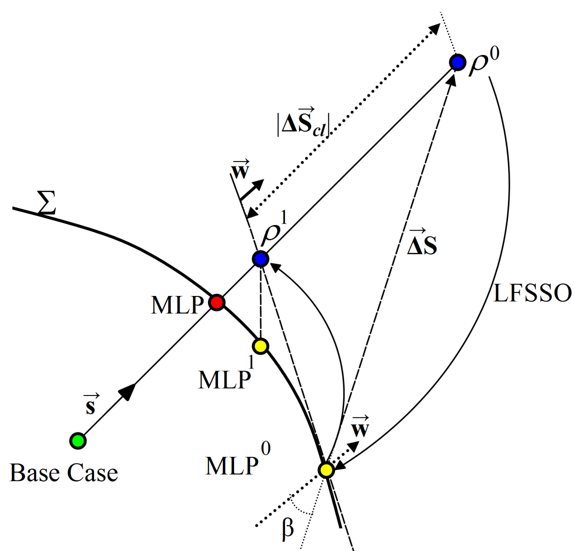

Figure 3.13: Process to obtain the MLP using the LFSSO.

According to (BEDRIÑANA AND CASTRO, 2008), the unit eigenvector ($\vec{\mathbf{w}}$), normal to the boundary Σ at the temporary critical point MLP^0 is computed. Then, a perpendicular plane, which is at the same time tangent to and intersects with the load increase direction, $\vec{\mathbf{s}}$, is computed. This point can be represented as

$$
\begin{aligned}
\vec{\mathbf{S}}^{new} &= \rho^1 \vec{\mathbf{S}}_{bc} \\
&= \left(\rho^0 - \Delta\rho\right) \vec{\mathbf{S}}_{bc} \\
\rho^1 \vec{\mathbf{S}}_{bc} &= \left(\rho^0 - \Delta\rho\right) \vec{\mathbf{S}}_{bc} \longleftrightarrow \rho^1 = \left(\rho^0 - \Delta\rho\right) \; .
\end{aligned}
\tag{3.20}
$$

The load curtailment $\left|\Delta\vec{\mathbf{S}}_{cl}\right|$ can be calculated as

$$
\Delta\vec{\mathbf{S}}_{cl} = \left\|\Delta\vec{\mathbf{S}}_{cl}\right\| \vec{\mathbf{s}} \, . \tag{3.21}
$$

The apparent power at MLP^0 is

$$
\vec{\mathbf{S}'} = \vec{\mathbf{S}^0} - \vec{\Delta\mathbf{S}} \, . \tag{3.22}
$$

Projecting $\vec{\Delta\mathbf{S}}$ over a tangent line perpendicular to $\vec{\mathbf{w}}$ and with β the angle between them, the following expression can be written.

$$
\vec{\Delta\mathbf{S}} \cdot \vec{\mathbf{w}} = \left\|\Delta\vec{\mathbf{S}}_{cl}\right\| \cos\left(\beta\right) \; . \tag{3.23}
$$

Angle β is also the angle between unit vectors $\vec{\mathbf{s}}$ and $\vec{\mathbf{w}}$, hence $\cos\left(\beta\right) = \vec{\mathbf{s}} \cdot \vec{\mathbf{w}}$ and

$$
\Delta\vec{\mathbf{S}}_{cl} = \frac{\vec{\Delta\mathbf{S}} \cdot \vec{\mathbf{w}}}{\cos\left(\beta\right)} \vec{\mathbf{s}} = \frac{\vec{\Delta\mathbf{S}} \cdot \vec{\mathbf{w}}}{\vec{\mathbf{s}} \cdot \vec{\mathbf{w}}} \vec{\mathbf{s}} \, . \tag{3.24}
$$

Recalling that $\vec{\mathbf{S}} = \left\|\vec{\mathbf{S}}\right\| \vec{\mathbf{s}}$ one gets

$$\Delta\rho = \frac{\left\|\vec{\Delta \mathbf{S}}\right\|}{\left\|\vec{\mathbf{S}}\right\|} = \frac{\vec{\Delta \mathbf{S}} \cdot \vec{\mathbf{w}}}{\vec{\mathbf{S}} \cdot \vec{\mathbf{w}}} . \tag{3.25}$$

3.3.2 Acceptable error margin

The method proposed in (DE LIMA TAVARES, 2010) uses the good characteristics of (BEDRIÑANA AND CASTRO, 2008) and adds some other interesting features:

- Includes practical information, generally defined by each company on the acceptable error in the final result for the MLP estimation.
- The performance of the proposed method does not depend on the choice of an infeasible operating point. Therefore, the choice of the initial ρ is not a critical issue.

For instance, some utility may define that "the acceptable error in ρ^{mlp} is 5%. Therefore, any value between $0.95\,\rho^{mlp}$ and $1.05\,\rho^{mlp}$ is considered as a good one for practical purposes, regarding monitoring and control. Figure 3.14 illustrates this idea using the well-known PV curve; it must be pointed out that this acceptable error margin is ideally of fixed width.

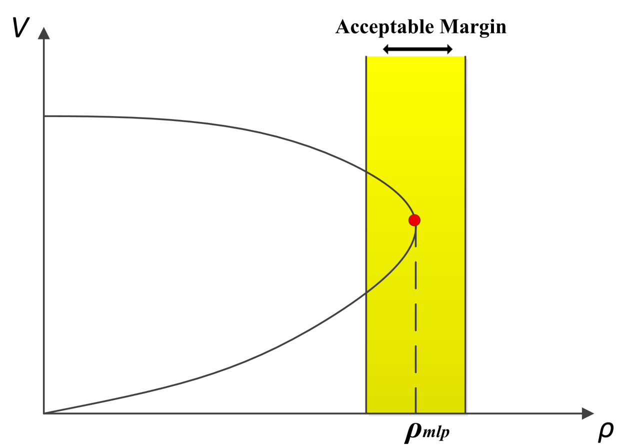

Figure 3.14: Acceptable error margin. Adapted from (XAVIER ET AL., 2013)

Parameter α can be calculated as

$$\alpha = \frac{\left(1 + \dfrac{x}{100}\right)}{\left(1 - \dfrac{x}{100}\right)} \tag{3.26}$$

The process to find the loading factor needed to take the base case to the MLP, $\hat{\rho}^{mlp}$ using the method discussed earlier is described as follows.

(1) Set counter $i = 0$. Set ρ^i.

(2) Run LFSSOP for ρ^i. If $\mu \to 0$ go to (3). Else, $\rho_{temp} = \rho^i$ and go to (5).

(3) Obtain $\rho_{temp} = \rho^i - \Delta\rho$. If $\rho_{temp} > 1$ go to (4). Else, $\rho_{temp} = 1$ and go to (4).

(4) Run LFSSOP for ρ_{temp}. If $\mu > 0$ continue. Else, (6).

(5) Run LFSSOP for $\rho^{i+1} = \alpha\, \rho_{temp}$. If $\mu \to 0$ then $\hat{\rho}^{mlp} = \left(\rho_{temp} + \rho^{i+1}\right)/2$, then End. Else, $\rho^{i+1} = \left(\rho^i + \rho^{i+1}\right)/2$, do $i = i + 1$ then go to (2).

(6) Run LFSSOP for $\rho^{i+1} = \alpha/\rho_{temp}$. If $\mu > 0$ $\hat{\rho}^{mlp} = \left(\rho_{temp} + \rho^{i+1}\right)/2$ then End. Else, $i = i + 1$ and go to (3).

Some possible situations that may be encountered in an iterative process by using the error margin are illustrated in Figure 3.15. From an operating point at iteration $(i-1)$, iteration i consists in using Eq. (3.25), leading to a new operating point. Points **A** (infeasible) and **D** (feasible) are unacceptable, since they are outside of the acceptable range. On the other hand, points **B** (infeasible) and **C** (feasible) are acceptable, since they are within the acceptable range.

Finally, keeping the stated definition the VSM can be calculated as

$$\text{VSM} = \hat{\rho}^{mlp} \tag{3.27}$$

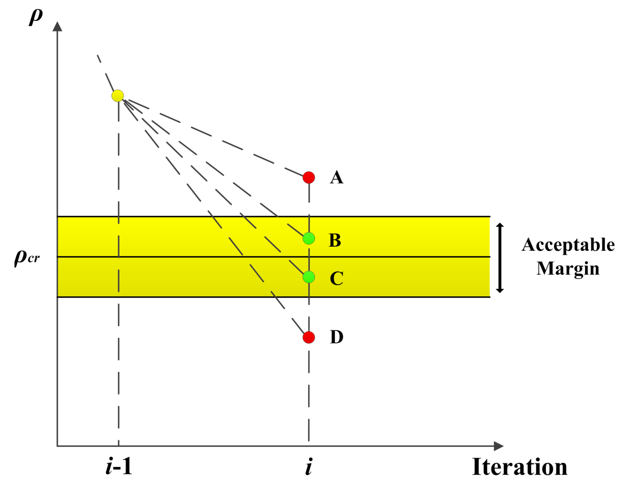

Figure 3.15: Illustration of the iterative process.

3.3.3 Example of the use of LFSSO for Voltage Stability

The same example system used for the initializing methods in section 3.1.4 will be used here using the method explained previously. The first step is to set the acceptable error margin, which in this case is arbitrary set at $x = 5\%$, and the initializing value $\rho^0 = 3$. The initializing value is in the infeasible region, as suggested in the algorithm, however it could hypothetically take any value.

Since $x = \pm 5\%$, (3.26) leads to

$$\alpha = \frac{\left(1 + \dfrac{5}{100}\right)}{\left(1 - \dfrac{5}{100}\right)} = 1.1053\,.$$

Following the algorithm results in

(1) $i = 0$, $\rho^0 = 3$ and $x = \pm 5\%$ ($\alpha = 1.1053$).

(2) Running LFSSO results in $\mu \to 0$ meaning that the current operating point is in the infeasible region. Go to (3).

(3) Compute $\rho_{temp} = \rho^i - \Delta\rho$, where

$$\Delta\rho = \frac{\vec{\Delta\mathbf{S}} \cdot \vec{\mathbf{w}}}{\vec{\mathbf{S}} \cdot \vec{\mathbf{w}}}$$

and $\vec{\mathbf{w}}$, $\vec{\Delta\mathbf{S}}$ and $\vec{\mathbf{S}}$ have to be calculated. $\vec{\mathbf{w}}$ is the left eigenvector associated to the minimum eigenvalue of the Jacobian matrix. $\vec{\Delta\mathbf{S}}$ is the difference between the power at the initial point and the power at the boundary surface, i.e. the mismatch vector, and $\vec{\mathbf{S}}$ is the power residuals in all network buses.

$$\vec{\mathbf{w}} = \begin{bmatrix} 0 \\ 0 \\ -0.8221 \\ -0.5402 \\ -0.1797 \\ -0.0000 \end{bmatrix}, \vec{\Delta\mathbf{S}} = \begin{bmatrix} 0 \\ 0 \\ -9.6322 \\ -6.2667 \\ 2.8076 \\ -1.8031 \end{bmatrix}, \vec{\mathbf{S}} = \begin{bmatrix} 0 \\ 0 \\ -7.1400 \\ -3.0600 \\ 2.0400 \\ 0 \end{bmatrix}$$

$$\Delta\rho = 1.5091 \quad \text{then} \quad \rho_{temp} = 3 - 1.5091 = 1.4909$$

Since $\rho_{temp} \geq 1$, then go to (4).

(4) Running LFSSO results in $\mu \to 0$. Then go to (6).

(6) Run LFSSO for $\rho^1 = \frac{1.4909}{1.1053} = 1.3489$. It results in $\mu \to 0$, then go to (3).

(3) $\rho_{temp} = \rho^1 - \Delta\rho$, where

$$\Delta\rho = \frac{\vec{\Delta\mathbf{S}} \cdot \vec{\mathbf{w}}}{\vec{\mathbf{S}} \cdot \vec{\mathbf{w}}}$$

$$\vec{\mathbf{w}} = \begin{bmatrix} 0 \\ 0 \\ -0.6200 \\ -0.7053 \\ -0.1120 \\ -0.3250 \end{bmatrix}, \vec{\Delta\mathbf{S}} = \begin{bmatrix} 0 \\ 0 \\ -1.4398 \\ -0.6271 \\ 0.5828 \\ -0.8819 \end{bmatrix}, \vec{\mathbf{S}} = \begin{bmatrix} 0 \\ 0 \\ -7.1400 \\ -3.0600 \\ 2.0400 \\ 0 \end{bmatrix}$$

$$\Delta\rho = 0.2448 \quad \text{then} \quad \rho_{temp} = 1.3489 - 0.2448 = 1.1041$$

Since $\rho_{temp} \geq 1$, then go to (4).

(4) Running LFSSO results in $\mu \rightarrow 0$. Then go to (6).

(6) Run LFSSO for $\rho^1 = \frac{1.1041}{1.1053} = 0.9989$. $\mu > 0$

$$\hat{\rho}^{mlp} = \frac{(1.1041 + 0.9989)}{2} = 1.0515$$

Finally, the VSM for the current operation point is

$$\text{VSM} = 1.0515$$

Meaning that the system has a margin of approximately 5% before reaching the MLP.

The values taken by the loading factor and the ideal error margin during the process can be seen in Figure 3.16. The estimated MLP lays within the error margin for this particular system. Unfortunately, under certain circumstances this result can be outside of the margin, basically because the theoretical value of the acceptable margin depends on the real system's MLP, which is not available. In fact, this is the unknown variable of interest. Nevertheless, the errors of these values outside of the acceptable margin are tolerable since they are due to numerical approximations in the LFSSO; as explained in (XAVIER, 2013).

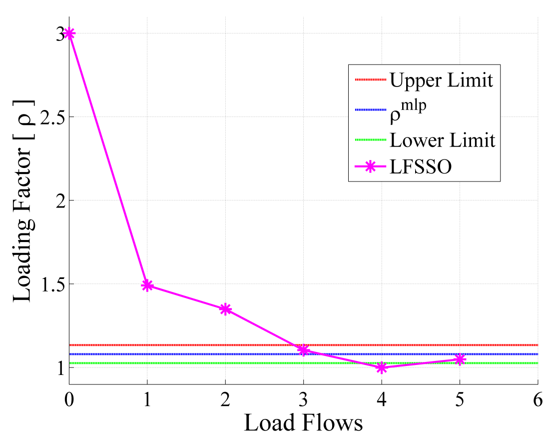

Figure 3.16: Behavior of the method LFSSO, 3-bus example system.

4 Proposed Methods

As stated before, the main objective of this work is to obtain an efficient method to estimate the MLP and the VSM of a system in real time, but at the same time, to be robust enough to be able to compute them with a low error margin. In order to do so, two methods based on the LFSSO are proposed using two different initializing methods to reduce the number of LFSSO runs performed. As could be seen in Chapter 3, both proposed Initializing Methods performed satisfactorily for the tested systems, showing a relative low mean error between the obtained margins and the values used as reference. However, they presented some problems for light load conditions, resulting in errors as discussed in the previous chapter.

On the other hand, the LFSSO for voltage stability analysis (explained in Section 3.3) has shown excellent results in previous works in terms of accuracy, when comparing the obtained values with the reference. Nevertheless, the number of iterations required for the method to reach these results was usually high, since high loading factors were generally used in order to show the robustness of the method, like in (BEDRIÑANA AND CASTRO, 2008), (TAVARES ET AL., 2009), (TAVARES ET AL., 2010), and (XAVIER ET AL., 2013). The conclusion is that the method shows excellent results no matter the initializing point is, however, the number of iterations required to reach an acceptable margin depends highly on its proximity to the actual MLP. Some efforts have been made in order to estimate more useful initializing values and hence to reduce the number of iterations as in (LI ET AL., 2010), yet, this method does not take reactive power generator's limits into account and the number of LFSSO performed was not reduced considerably.

4.1 Proposed Method I: Initializing Method 1 + LFSSO

In this proposed method the *Initializing Method 1* is used to provide an initial loading factor for the LFSSO. As explained in Section 3.1.2 the *Initializing Method 1* proposes the calculation of the MLP of one single bus named *weakest bus* after several calculations based on the CSE technique for all load buses. The initializing value, $\rho_1^{ini} = \text{VSM}_1$, is then used as the initial loading factor for the LFSSO for voltage stability analysis in Section 3.3 and the loading factor to reach the system to the MLP ($\hat{\rho}_1^{mlp}$) can be calculated. Finally, the VSM can be calculated as explained in Section 3.3.

The method's flow chart is shown in Figure 4.1.

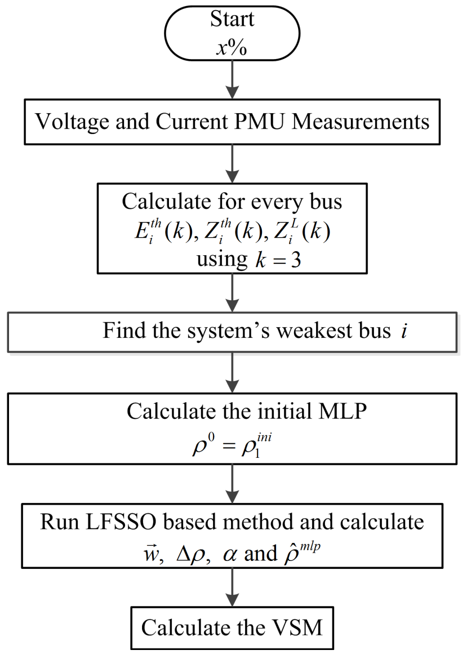

Figure 4.1: Proposed Method I Flowchart.

4.2 Proposed Method II: Initializing Method 2 + LFSSO

As explained before, the idea of using initializing methods as input variables of the LFSSO is to improve the general method's computational burden by reducing the number of calculations. It can be assumed that if closer values to the actual MLP are used, then lesser LFSSO runs must be performed.

When comparing the mean error value for the tested initializing methods in Section 3.2 for both test cases, it could be seen that the *Initializing Method 2*shows smaller error mean values for almost all tested systems, indicating that the obtained MLP was closer to the reference value. As explained in Section 3.1.3, *Initializing Method 2* not only takes into account the weakest bus of the system, but also calculates the MLP using the information of a set of critical buses depending on a threshold parameter γ, which helps on filtering out the not so representative buses.

Again, as in the **Proposed Method I**, the initializing value, $\rho_2^{ini} = \text{VSM}_2$, is used as the initial loading factor for the LFSSO based method to calculate the MLP and $\hat{\rho}_2^{mlp}$. Then, the VSM can be calculated as in Section 3.3.

The method's flow chart is shown in Figure 4.2.

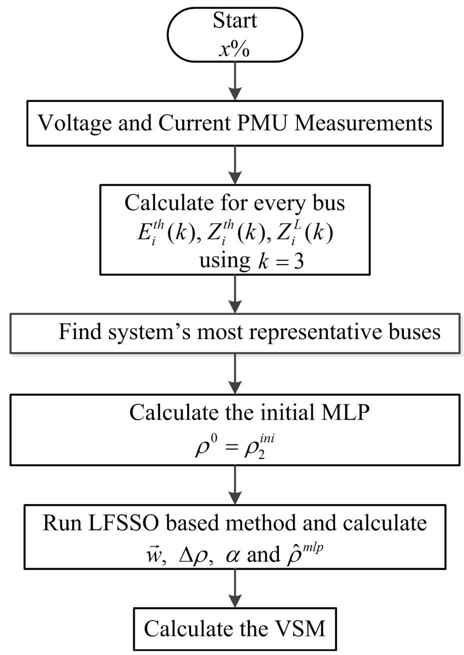

Figure 4.2: Proposed Method II Flowchart.

4.3 Example using the Proposed Methods

The same example system used in previous sections will be used here. The tolerance is $x = \pm 5\%$, since the same system was used in Section 3.1.4 for testing the initializing methods. The values of the VSM found there are used as initial loading factors ρ^0. As explained there, $\mathrm{VSM}_1 = \mathrm{VSM}_2$ since there is only one load bus, hence, $\rho^0 = \mathrm{VSM}_1 = 1.3177$.

Since $x = \pm 5\%$, (3.26) one has

$$\alpha = \frac{\left(1 + \dfrac{5}{100}\right)}{\left(1 - \dfrac{5}{100}\right)} = 1.1053\,.$$

Following the proposed algorithm results in the steps shown next.

(1) $i = 0$, $\rho^0 = 1.3177$ and $x = \pm 5\%$ ($\alpha = 1.1053$).

(2) Running LFSSO results in $\mu \to 0$ meaning that the current operating point is in the infeasible region. Go to (3).

(3) Compute $\rho_{temp} = \rho^i - \Delta\rho$, where

$$\Delta\rho = \frac{\vec{\Delta \mathbf{S}} \cdot \vec{\mathbf{w}}}{\vec{\mathbf{S}} \cdot \vec{\mathbf{w}}}$$

$$\vec{\mathbf{w}} = \begin{bmatrix} 0 \\ 0 \\ 0.6153 \\ 0.7109 \\ 0.1081 \\ 0.3229 \end{bmatrix}, \vec{\Delta \mathbf{S}} = \begin{bmatrix} 0 \\ 0 \\ -1.2642 \\ -0.4811 \\ 0.5526 \\ -0.9130 \end{bmatrix}, \vec{\mathbf{S}} = \begin{bmatrix} 0 \\ 0 \\ -7.1400 \\ -3.0600 \\ 2.0400 \\ 0 \end{bmatrix}$$

$$\Delta\rho = 0.2134 \quad \text{then} \quad \rho_{temp} = 1.3177 - 0.2134 = 1.1043$$

Since $\rho_{temp} \geq 1$, then go to (4).

(4) Running LFSSO results in $\mu \to 0$. Then go to (6).

(6) Run LFSSO for $\rho^1 = \frac{1.1043}{1.1053} = 0.9991$. It results in $\mu > 0$, then

$$\hat{\rho}^{mlp} = \frac{(1.1043 + 0.9991)}{2} = 1.0517$$

Finally, the VSM for the current operation point is 1.0517, meaning that the system has a margin of approximately 5% before reaching the MLP.

The values taken by the loading factor and the ideal error margin during the process can be seen in Figure 4.3. As expected, the estimated MLP lays within the error margin. It could be seen that the number of LFSSO required this time are less than those needed in Section 3.3.3 and the final result is quite similar (approximately 5%).

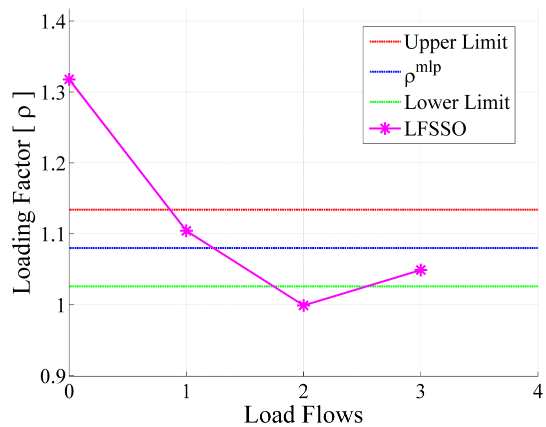

Figure 4.3: Behavior of the method for the 3-bus example system.

4.4 Tests and Results

The proposed methods were tested for the IEEE 14, 30, 57 and 118-bus test systems, and for a realistic Brazilian transmission system with a total of 4,526 buses, 500 synchronous machines with 64.78 GW of total generation, and a base load of 61.47 GW and 20.46 GVAr. All generators and loads were modified by a scale factor (λ_i) in periods of one hour in order to simulate a daily load curve, deliberately driving each system relatively near to its MLP. Random values with a coefficient of variation $CV = 2\%$ following a normal distribution were added to the daily load curve for every load and generator and for every sample, so a more realistic scenario was obtained. The value of γ for the initializing method 2 was set at 0.5, the acceptable error $x = \pm 2\%$, and the tolerance for the LFSSO and for the optimal multiplier was set to 0.01 pu. Generator reactive power limits were enforced. The results obtained with the proposed methods were compared with those after running successive power flows increasing the loading factor until it did not converge, and was named Reference Method (*ref*). All results were obtained after running 500 random loading cases with the characteristics explained before since random variables are used. An illustration of this can be seen in Fig.4.4, where four different loading cases are shown (dashed lines) together with its respective mean value (continuous line) for a particular system.

Once the MLP has been found using the initializing methods, it is straightforward to calculate the VSM using the procedure shown above, again for a period of 24 hours in intervals of one hour. The VSM of the IEEE 118-bus test system and the BR 4,526-bus system during a day are shown in Figure 4.5 $a)$ and $b)$ respectively. The margins obtained using only the initializing methods can

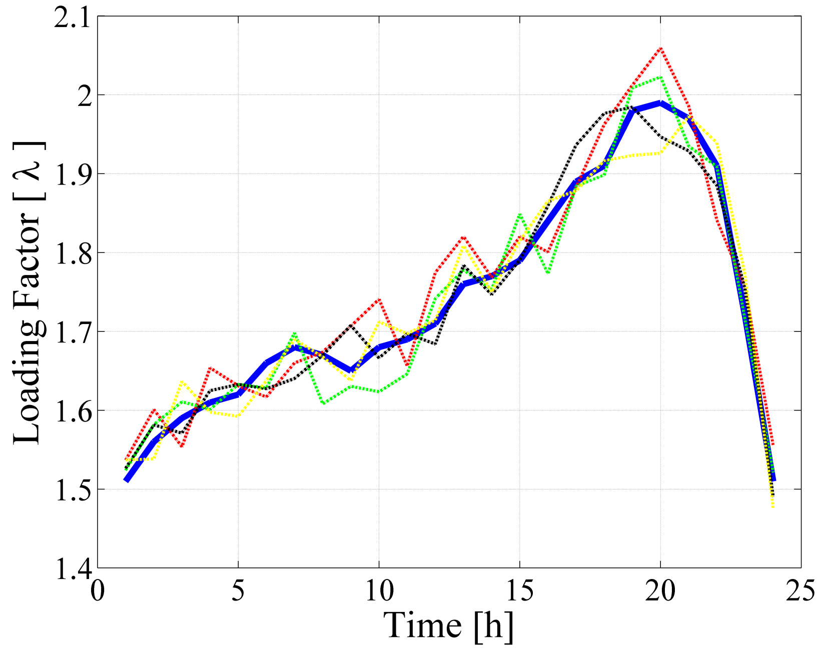

Figure 4.4: Different loading cases for a particular system.

be compared with those using the proposed methods and the reference, which was obtained after running successive power flows for a particular daily load case. Similarly, the VSM of the IEEE 30-bus and 57-bus test systems are shown in Figure 4.6 $a)$ and $b)$ respectively.

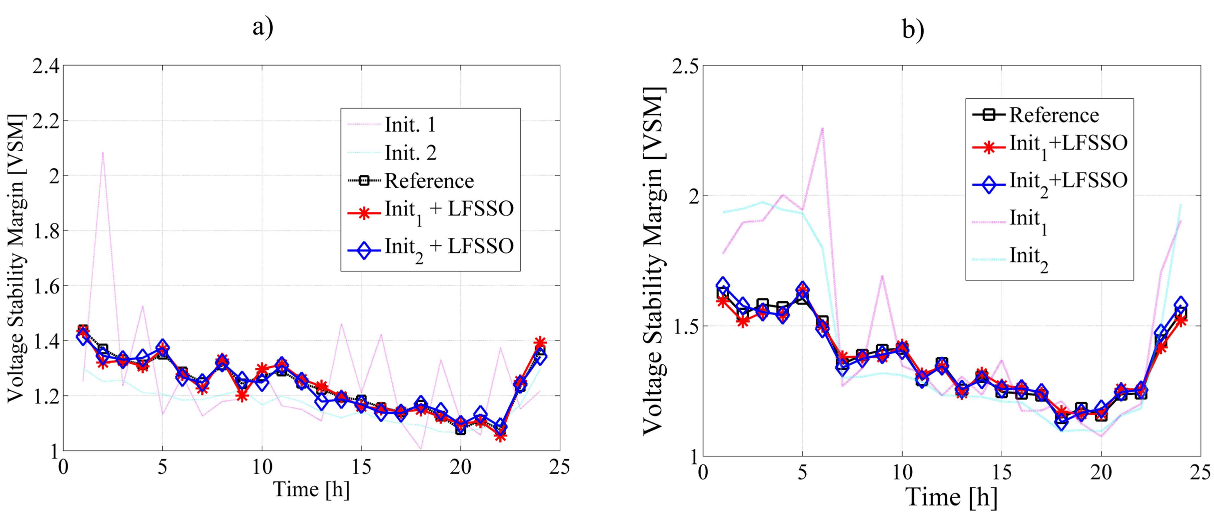

Figure 4.5: VSM using different methods. a) 118-bus b) BR 4,526-bus system.

The initializing methods provide good first estimates of the VSM, however, as discussed before, they may present higher errors, basically depending on the system's current conditions and

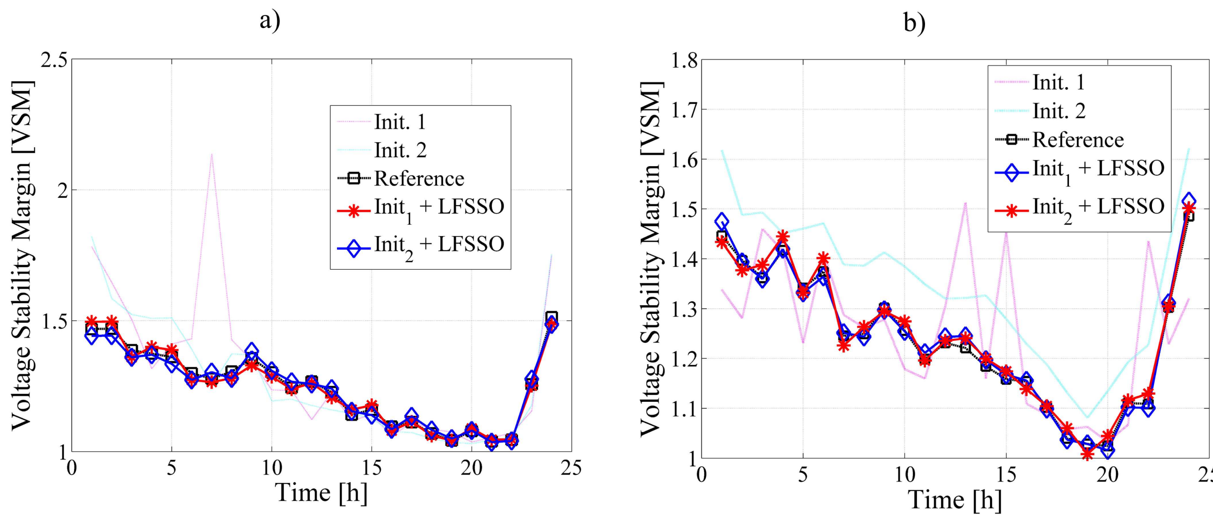

Figure 4.6: VSM using different methods. a) 30-bus b) 57-bus system.

on the estimated TE. When the initializing methods are used as initial values for the LFSSO based method, the estimated VSM gets closer to the reference value. In fact, the average values of the VSM obtained using only the initializing methods and using the proposed methods, as well as the average of the errors on the estimated VSMs, calculated as in Eq.3.17 and Eq.3.18 are shown in Table 4.1 for all tested systems.

The errors resulting from the proposed method showed to be reduced if compared with those obtained when only the initializing methods are used to estimate the VSM. It is an intuitive result, since the LFSSO based method had previously shown outstanding results. Nevertheless, it must be highlighted that these results where obtained with fewer number of LFSSO calculations, considering that the initial value of ρ was previously estimated.

In order to show the actual reduction on the number of routines performed applying the method, Figure 4.7 shows the number of LFSSO for every hour during a period of 24 hours for the IEEE 57-bus and 118-bus test systems. These values were obtained using both initializing methods proposed (ρ_1^{ini} and ρ_2^{ini}) as the initial loading factor ρ^0 for the LFSSO, again only for one particular loading case. Similarly in Figure 4.8 the number of LFSSO performed are shown for the IEEE 30-bus test system and for the Brazilian transmission system of 4,526 buses.

The approximated average values of the total number of LFSSO performed using the proposed methods are also shown in Table 4.2. These values can be compared with the number of LFSSO

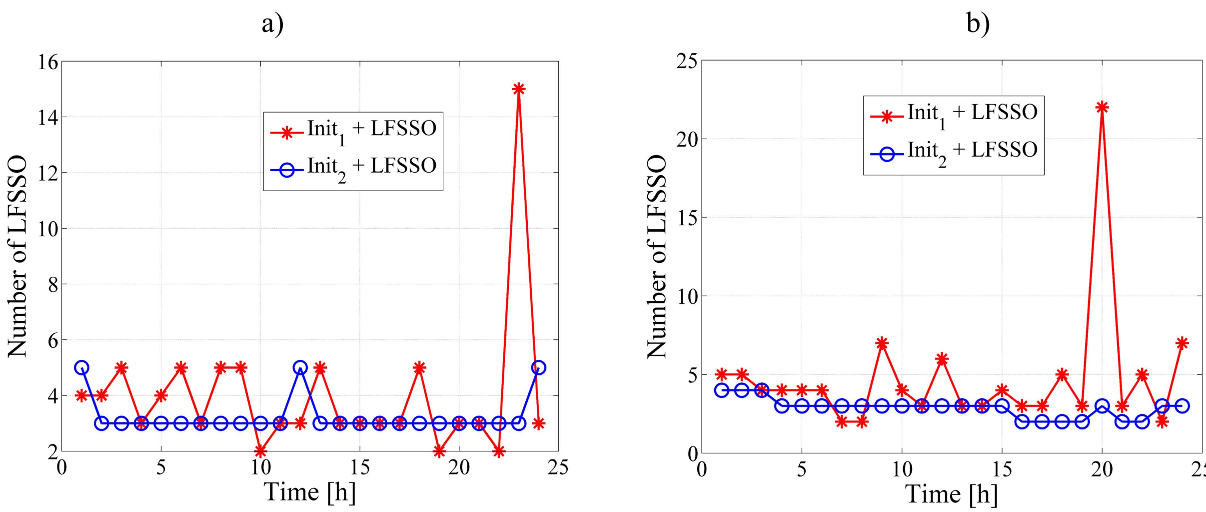

Figure 4.7: Number of LFSSO performed. a) 57-bus b) 118-bus.

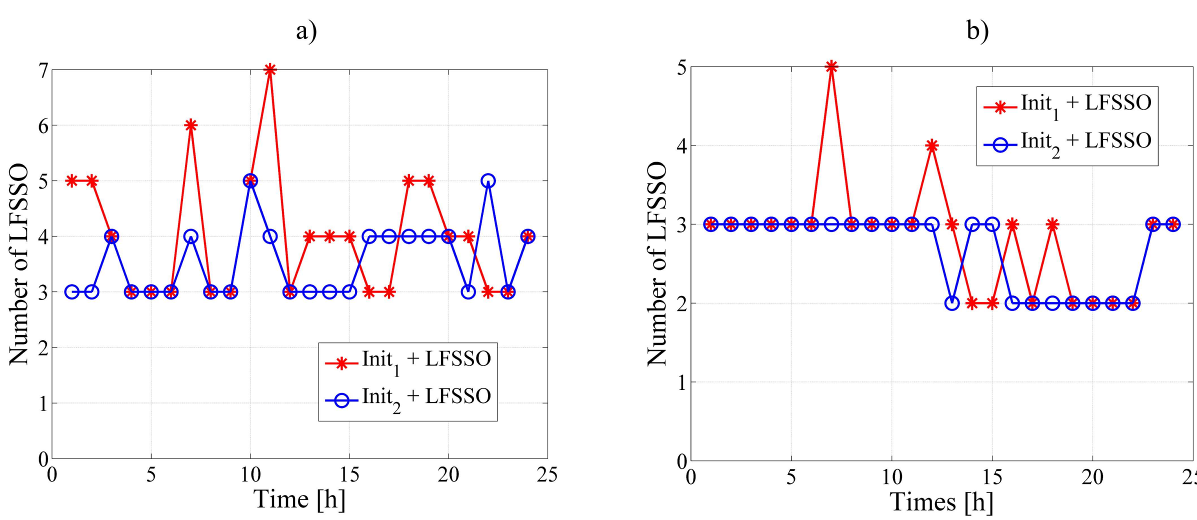

Figure 4.8: Number of LFSSO performed. a) 4526-bus b) 30-bus.

Table 4.1: VSM using different calculation methods

System VSM[a]		Initia.$_1$	Initia.$_2$	I$_1$+LFSSO	I$_2$+LFSSO
IEEE 14-bus	VSM	1.2990	1.2919	1.3768	1.3701
1.3756	$\varepsilon\%$	18.23	9.74	2.10	2.31
IEEE 30-bus	VSM	1.2823	1.2820	1.2407	1.2437
1.2441	$\varepsilon\%$	15.76	5.38	1.50	1.35
IEEE 57-bus	VSM	1.2465	1.2463	1.2440	1.2388
1.2368	$\varepsilon\%$	9.14	8.69	2.47	2.02
IEEE 118-bus	VSM	1.0456	1.1132	1.2340	1.2312
1.2291	$\varepsilon\%$	5.02	4.49	3.01	3.13
BR 4526-bus	VSM	1.2165	1.2709	1.3333	1.3414
1.3595	$\varepsilon\%$	2.35	2.33	1.12	1.01

[a]Voltage stability margin obtained with successive load flows (mean value).

performed after choosing an arbitrary value in the infeasible region ($\rho_r^0 = 10$). This value was chosen since it has already been used in previous works as in (BEDRIÑANA AND CASTRO, 2008) and (TAVARES ET AL., 2010). The mean value of the loading factor that takes the system to the MLP ($\hat{\rho}^{mlp}$) calculated using the proposed methods are also shown for the used initial loading factors and can be compared with the reference, ρ^a for every tested system.

From Figure 4.7 and Figure 4.8 it could be seen that the number of LFSSO performed using the *Initializing Method 2* was usually less than using the *Initializing Method 1*, especially on the latest hours for the IEEE 57-bus and 118-bus test systems where outlier values can be seen. However, these graphics show only a particular loading case and the mean values in Table 4.2 (using 500 random loading cases) indicate that even though the average number of LFSSO performed using the *Initializing Method 2* were less than using the *Initializing Method 1* the main advantage of using either of the proposed initializing methods is when compared to the results obtained using the arbitrarily chosen value $\rho_r^0 = 10$. It can be seen that the number of routines performed were considerably reduced, almost 40% in the worst case (BR 4525-bus using the *Initializing Method 1*) and up to 72% in the best case (IEEE 57-bus test system using the *Initializing Method 2*). When comparing the values of the critical loading factor, $\hat{\rho}^{mlp}$, it can be seen that all results lay inside of

Table 4.2: MLP using different initializing values

System ρ^a		ρ_1^{ini}	ρ_2^{ini}	ρ_r^0
IEEE 14-bus 1.7830	ρ^0	1.7768	1.6811	10
	$\hat{\rho}^{mlp}$	1.7897	1.7849	1.7486
	# LFSSO.	4	3	7
IEEE 30-bus 1.5299	ρ^0	1.5932	1.5546	10
	$\hat{\rho}^{mlp}$	1.5320	1.5236	1.5032
	# LFSSO.	3	3	7
IEEE 57-bus 1.6170	ρ^0	1.7331	1.7063	10
	$\hat{\rho}^{mlp}$	1.6201	1.6258	1.6145
	# LFSSO.	6	3	11
IEEE 118-bus 2.1446	ρ^0	1.8571	1.9465	10
	$\hat{\rho}^{mlp}$	2.1348	2.1326	2.1021
	# LFSSO.	5	4	13
BR 4,526-bus 1.3390	ρ^0	1.3143	1.2817	10
	$\hat{\rho}^{mlp}$	1.3302	1.3283	1.2795
	# LFSSO.	5	4	8

[a] Loading factor obtained for the original case (original data) with successive load flows.

the acceptable margin (2%) but the one obtained using $\rho_r^0 = 10$ for the IEEE 118-bus test system, where the mean error was 4.4%, suggesting that several samples may had exceeded the acceptable error margin.

The iterative processes of finding the MLP for a particular loading case for the 118-bus and 57-bus test systems are shown in Figure 4.9 $a)$ and $b)$ respectively and for the IEEE 14-bus test system and the Brazilian transmission system in Figure 4.10. All of them were obtained using the system's initializing values in Table 4.2. For the sake of clarity, it is worth mentioning that the number of load flow calculations do not strictly match with the ones of Table 4.2 since, as explained before, only average values were shown in it. Nevertheless, it is a good example of how the method responds to different initial values and the effect of using the proposed initializing methods. It is clear that the method becomes significantly more efficient if the initial values get closer to the actual

MLP.

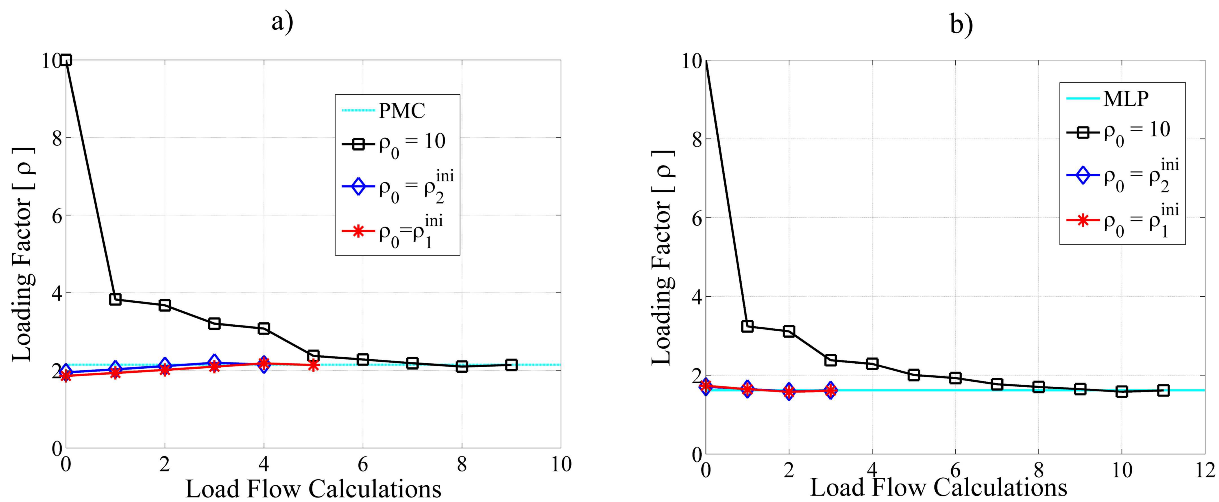

Figure 4.9: MLP process with different initial loading factors. a) IEEE 118-bus b) IEEE 57-bus.

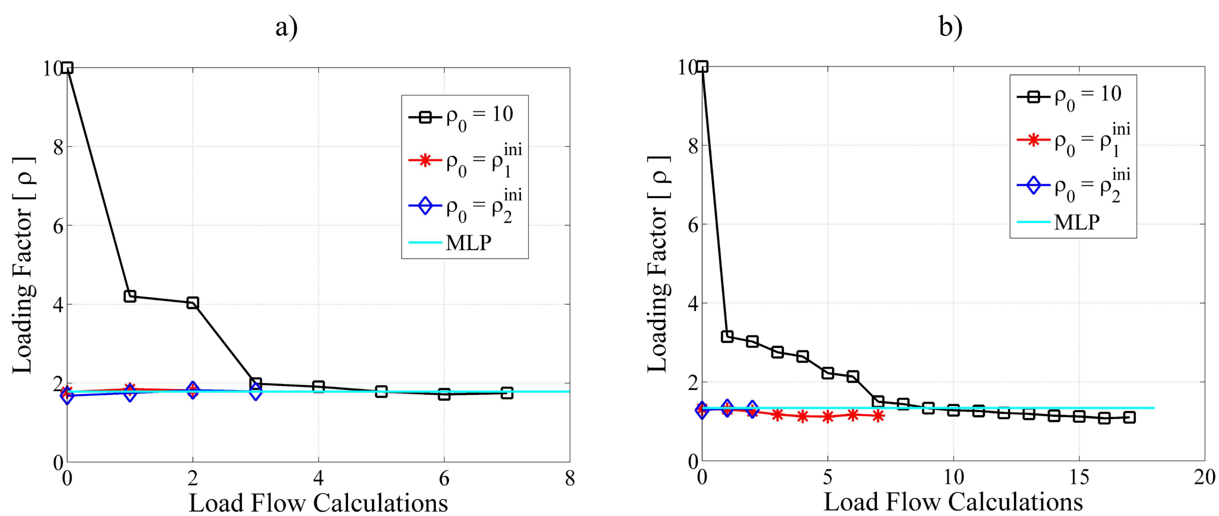

Figure 4.10: MLP process with different initial loading factors. a) IEEE 14-bus b) BR 4526-bus.

Again, it can be seen that the number of LFSSO performed is considerably reduced when using either of the proposed methods (using the initializing methods) for all tested systems. Note that the number of LFSSO to find the MLP is dependent on the initial point, one should think that the number of calculations decreases when values closer to the MLP are used. However, even though this happens in most cases, there are some others like the case of Figure 4.9 b) for the IEEE 57-bus test system where slight differences in initial values do not make any difference in the total number of LFSSO performed or other cases where the closer initializing value produces an increase in the number of routines as Figure 4.10 b) for the Brazilian transmission system. This might happen because of the variable acceptable margin, explained in Section 3.3.2, since the calculated values depend in some cases of this margin.

5 Conclusions and Future work

The main idea of this work was to obtain a method to estimate the VSM of a network using phasor measurements. This method had to be efficient enough so as to be implemented in real time environments, but sufficiently robust to give a good estimate of the system's proximity to the MLP and a reliable value to the network operator. In order to do so, a combination of two voltage stability assessment methods was proposed. The first method was a variation of a previously presented one (SU ET AL., 2012), based on local measurements and Thevenin equivalents as seen from all measured buses. Two different variations were presented, and were named "Initializing Methods", which showed to behave relatively well when compared with the previously mentioned similar method, especially for heavy loading conditions, that is, closer to the MLP. However, the proposed initializing methods presented some drawbacks under light load conditions and when the system was subject to significant disturbances between samples, producing a poorer estimate of the Thevenin equivalent circuit and therefore of the VSM. To overcome these problems, the use of a second method was proposed, based on the LFSSO (XAVIER ET AL., 2013) which would use the VSM provided by the initializing methods as an input variable, in order to reduce the number of iterations required to converge.

5.1 Conclusions

The first initializing method proposed uses the CSE to estimate the MLP by extrapolating a current operational condition using the Thevenin equivalent and voltage and current measurements. After this estimate is obtained, a second calculation of the MLP is performed analytically, this time only for the weakest bus, as explained in Section 3.1.2. Similarly, the second proposed method uses the information of the Thevenin equivalent and bus measurements to calculate the MLP analytically for every measured bus, this time without using the CSE at any moment. After computing the MLP of every bus, a weighting factor is assigned to each one and compared with a threshold that works like a filter selecting only the most critical buses, reducing the sensitivity of the method to estimate errors and indirectly controlling the number of buses used to calculate the VSM.

Both initializing methods were tested using well-known IEEE test systems and a part of the real Brazilian bulk transmission system, by applying two different tests to evaluate their performance. The first one considers the same loading factor for all buses and a controlled time criteria between samples. The second test considered random behavior in the loading factor of each bus as in the time criteria, as an attempt to simulate a more realistic case, where taken samples are not controlled by power changes but by time lapse, taking the loading factors used in the first test as mean values and a defined coefficient of variation. It could be seen that the results obtained using only the initializing methods were relatively good, considering their simplicity and that they are only based on local measurements. However, as said before, several circumstances can reduce the effectiveness of the methods, such as significant changes in the rest of the system between samples, either in topology or because of considerable changes in the operation point, including lack of information about the amount of reactive power reserves and the effect of generators reaching their capability limits, system contingencies, and so on.

The evaluation of the proposed methods was also performed using the same test systems and the bulk Brazilian system. Only the characteristics of the second test used for the initializing methods were used (random loading factors and time criteria). The number of LFSSOs performed using the initializing methods were compared with the ones using an arbitrarily set initializing loading factor, and the VSM obtained, compared with the one after running successive power flows until it did not converge. The process was performed 500 times in order to obtain a tendency. It could be seen that the number of LFSSO required to obtain the VSM using the proposed methods was considerably reduced compared when using the arbitrary value, maintaining a good estimation of the VSM. This reduction on the number of routines means a decrease in the computational effort and consequently in the computation time, which is one of the main objectives for real time applications.

It should also be pointed out that the proposed methods not only indicate the VSM of the system, but also its most critical buses. Depending on the method used, it was shown that the number of critical buses changed considerably, since the **Proposed Method I** only takes the most critical bus and the **Proposed Method II** a set of buses that depend on the system's behavior and are controlled by the specified threshold (γ). However, it was shown that no matter the initializing method used, the final result was very accurate and the difference between the number of LFSSO using either of the initializing methods was not significant, at least for the tested systems and under the specified operation points. This means that there would not be an apparent advantage of using the **Proposed Method II** since it requires the utilization of information from more buses and no advantage in terms of accuracy or reduction in the number of LFSSO. Nonetheless, it should be noticed that the MLP of all measured buses must be calculated since the weakest bus or buses must be chosen form all of them, no matter which initializing method is used.

After running a considerable number of simulations, it was perceived that the difference between the number of chosen buses (critical buses) for different operation points was not considerable from one point to another. This means that the systems behaved almost the same, at least in terms of critical buses for changing loading factors. This result could be of high interest from and economical and a network operator point of view, since only information from critical buses could be used and provide an good view of the network, decreasing the number of buses that must be monitored and eventually controlled. One should not forget that even though the results given in this work were obtained for intervals of one hour, one of the main advantages of PMUs is their data sampling rate. Hence, in real time environments there would be several VSM estimations every hour, even every minute if required, so the knowledge of critical buses could help in the fast identification of possible alert situations. This means that it is very important to choose the right set of critical buses, both, for economical and technical issues, and the possibility of choosing a set of critical buses by the right set of γ in a method like the **Proposed Method II** could be more attractive when compared with the **Proposed Method I**.

5.2 Future Work

During the development of this work, several ideas came up that could complement the presented methods or use them as a part of additional routines.

As mentioned before, the main advantages of PMUs are their fast, accurate, continuous, and time synchronized data sampling from virtually any quantities in the system. One possible future work is to obtain the VSM with the proposed method using real PMU measured data, calculating the margin more frequently, for example, once every ten minutes, every minute and so on, and estimate what time lapse would be more appropriate for different systems.

Another possible idea for future work is to implement an additional method that provides updated information of local reactive reserves to the initializing methods. This could probably reduce the estimation errors for light load scenarios and enhance the method.

Finally, the effect and the right choice of the threshold parameter γ for the Initializing method 2 is another aspect that must be studied in more detail for future works.

5.3 Publications

The results of this research were accepted for publication in:

- Giraldo, J. S., Castrillon, J. A. and Castro, C. A., "Network-Free Voltage Stability Assessment of Power Systems using Phasor Measurements", IEEE PowerTech Eindhoven 2015, 29 June - 02 July, Eindhoven, The Netherlands.
- Giraldo, J. S., Castrillon, J. A. and Castro, C. A., "Robust and Efficient Voltage Stability Margin Computation using Synchrophasors", IEEE 2015 Power and Energy Society General Meeting, 26-30 July, Denver, USA.
- Giraldo, J. S., Castrillon, J. A. and Castro, C. A., "Avaliação em Tempo Real da Estabilidade de Tensão em Sistemas de Potência usando Medições Fasoriais", XXIII Seminário Nacional de Produção e Transmissão de Energia Elétrica, Foz do Iguaçu, PR, Brasil, 18-21 Outubro, 2015.

References

Abdelkader, S. M. and Morrow, D. J. (2012). Online tracking of Thévenin equivalent parameters using PMU measurements. *Power Systems, IEEE Transactions on*, 27(2):975–983.

Ajjarapu, V. and Christy, C. (1992). The continuation power flow: a tool for steady state voltage stability analysis. *Power Systems, IEEE Transactions on*, 7(1):416–423.

Alves, D., Da Silva, L., Castro, C., and da Costa, V. (2000). New parameterization schemes for the continuation load flow method. In *Electric Utility Deregulation and Restructuring and Power Technologies, 2000. Proceedings. DRPT 2000. International Conference on*, pages 179–184. IEEE.

Arones, M. F. B. (2010). *Desenvolvimento de uma metodologia robusta e eficiente para fluxo de carga da continuação otimo multiobjetivo*. PhD thesis, Universidade Estadual de Campinas (UNICAMP). Faculdade de Engenharia Elétrica e de Computação.

Bedriñana, M. F. and Castro, C. A. (2008). Maximum loading point computation based on load flow with step size optimization. In *Power and Energy Society General Meeting-Conversion and Delivery of Electrical Energy in the 21st Century, 2008 IEEE*, pages 1–8. IEEE.

Bijwe, P. and Kelapure, S. (2003). Nondivergent fast power flow methods. *Power Systems, IEEE Transactions on*, 18(2):633–638.

Boor, C. D. (1978). *A practical guide to splines*, volume 27. Springer Verlag, ISBN 978-0-387-95366-3.

Braz, L. M., Castro, C. A., and Murati, C. (2000). A critical evaluation of step size optimization based load flow methods. *Power Systems, IEEE Transactions on*, 15(1):202–207.

Candelo, J. E., Caicedo, G., and Castro, F. (2008). Métodos para el estudio de la estabilidad de voltaje en sistemas de potencia. *Información tecnológica*, 19(5):97–110.

Canizares, C. A. and Alvarado, F. L. (1993). Point of collapse and continuation methods for large ac/dc systems. *Power Systems, IEEE Transactions on*, 8(1):1–8.

Cañizares, C. A., Alvarado, F. L., DeMarco, C. L., Dobson, I., and Long, W. F. (1992). Point of collapse methods applied to ac/dc power systems. *Power Systems, IEEE Transactions on*, 7(2):673–683.

Canizares, C. A. et al. (2002). Voltage stability assessment: concepts, practices and tools. *Power System Stability Subcommittee Special Publication IEEE/PES, Final Document (thunderbox. uwaterloo. ca/˜ claudio/claudio. html# VSWG)*.

Castro, C. and Braz, L. (1997). A new approach to the polar newton power flow using step size optimization. In *Proceedings of the 29th North American Symposium, Laramie, Wyoming, USA*.

Chao, X., Austria, R., Reppen, N., Welsh, D., Uhrin, J., and Shultz, J. (1995). Practical determination of operating transfer limits. In *Power Industry Computer Application Conference, 1995. Conference Proceedings., 1995 IEEE*, pages 271–277. IEEE.

Chiang, H.-D., Flueck, A. J., Shah, K. S., and Balu, N. (1995). Cpflow: A practical tool for tracing power system steady-state stationary behavior due to load and generation variations. *Power Systems, IEEE Transactions on*, 10(2):623–634.

Committee, E. et al. (2012). Report of the enquiry committee on grid disturbance in northern region on 30th july 2012 and in northern, eastern & north-eastern region on 31st july, 2012.

Corsi, S. and Taranto, G. N. (2008). A real-time voltage instability identification algorithm based on local phasor measurements. *Power Systems, IEEE Transactions on*, 23(3):1271–1279.

Das, S. (2014). *Algorithms to Improve Performance of Wide Area Measurement Systems of Electric*

Power Systems. PhD thesis, The University of Western Ontario.

Dasgupta, S., Paramasivam, M., Vaidya, U., and Ajjarapu, V. (2012). Pmu-based model-free approach for short term voltage stability monitoring. In *Power and Energy Society General Meeting, 2012 IEEE*, pages 1–8. IEEE.

de Lima Tavares, B. (2010). Computing the maximum loading point in power systems based on load flow with step size optimization. Master's thesis, State University of Campinas.

Decker, I., Dotta, D., Agostini, M., Zimath, S., and de Silva, A. (2006). Performance of a synchronized phasor measurements system in the brazilian power system. In *Power Engineering Society General Meeting, 2006. IEEE*, pages 8–pp. IEEE.

Decker, I. C., Agostini, M. N., Prioste, F. B., Mayer, B. T., Dotta, D., et al. (2011). Experience and applications of phasor measurements to the brazilian interconnected power system. *European Transactions on Electrical Power*, 21(4):1557–1573.

Dehnel, M. and Dommel, H. (1989). A method for identifying weak nodes in nonconvergent load flows. *Power Systems, IEEE Transactions on*, 4(2):801–807.

Dobson, I. (1994). The irrelevance of load dynamics for the loading margin to voltage collapse and its sensitivities. In *Bulk power system voltage phenomena III, voltage stability, security & control, Proceedings of the ECC/NSF workshop, Davos, Switzerland*.

Dobson, I. and Lu, L. (1993). New methods for computing a closest saddle node bifurcation and worst case load power margin for voltage collapse. *Power Systems, IEEE Transactions on*, 8(3):905–913.

Dobson, I., Lu, L., and Hu, Y. (1991). A direct method for computing a closest saddle node bifurcation in the load power parameter space of an electric power system. In *Circuits and Systems, 1991., IEEE International Sympoisum on*, pages 3019–3022. IEEE.

Force, U.-C. P. S. O. T., Abraham, S., Dhaliwal, H., Efford, R. J., Keen, L. J., McLellan, A., Manley, J., Vollman, K., Diaz, N. J., Ridge, T., et al. (2004). *Final report on the august 14, 2003 blackout in the united states and canada: Causes and recommendations*. US-Canada Power System Outage Task Force.

Gao, B., Morison, G., and Kundur, P. (1996). Towards the development of a systematic approach for voltage stability assessment of large-scale power systems. *IEEE transactions on power systems*, 11(3):1314–1324.

Glavic, M. and Van Cutsem, T. (2011). A short survey of methods for voltage instability detection. In *Power and Energy Society General Meeting, 2011 IEEE*, pages 1–8. IEEE.

Gubina, F. and Strmcnik, B. (1995). Voltage collapse proximity index determination using voltage phasors approach. *Power Systems, IEEE Transactions on*, 10(2):788–794.

Gutierrez, J. F., Bedriñana, M. F., and Castro, C. A. (2011). Critical comparison of robust load flow methods for ill-conditioned systems. In *PowerTech, 2011 IEEE Trondheim*, pages 1–6. IEEE.

Hajagos, L. M. and Danai, B. (1998). Laboratory measurements and models of modern loads and their effect on voltage stability studies. *Power Systems, IEEE Transactions on*, 13(2):584–592.

Haque, M. (2003). On-line monitoring of maximum permissible loading of a power system within voltage stability limits. *IEE Proceedings-Generation, Transmission and Distribution*, 150(1):107–112.

Holbert, K. E., Heydt, G. T., and Ni, H. (2005). Use of satellite technologies for power system measurements, command, and control. *Proceedings of the IEEE*, 93(5):947–955.

Iba, K., Suzuki, H., Egawa, M., and Watanabe, T. (1991). Calculation of critical loading condition with nose curve using homotopy continuation method. *Power Systems, IEEE Transactions on*, 6(2):584–593.

Ibsais, A. and Ajjarapu, V. (1996). Voltage stability-limited interchange flow. *Electric power systems research*, 38(2):91–95.

Irisarri, G., Wang, X., Tong, J., and Mokhtari, S. (1997). Maximum loadability of power systems using interior point nonlinear optimization method. *Power Systems, IEEE Transactions on*, 12(1):162–172.

Iwamoto, S. and Tamura, Y. (1981). A load flow calculation method for ill-conditioned power systems. *Power Apparatus and Systems, IEEE Transactions on*, pages 1736–1743.

Jenkins, N., Allan, R., Crossley, P., Kirschen, D., and Strbac, G. (2008). *Embedded Generation*. The Institution of Engineering and Technology, London, United Kingdom.

Julian, D., Schulz, R., Vu, K., Quaintance, W., Bhatt, N., and Novosel, D. (2000). Quantifying proximity to voltage collapse using the voltage instability predictor (vip). In *Power Engineering Society Summer Meeting, 2000. IEEE*, volume 2, pages 931–936. IEEE.

Kessel, P. and Glavitsch, H. (1986). Estimating the voltage stability of a power system. *Power Delivery, IEEE Transactions on*, 1(3):346–354.

Kundur, P., Balu, N. J., and Lauby, M. G. (1994). *Power system stability and control*, volume 7. McGraw-hill New York, ISBN 978-0070359581.

Kundur, P., Paserba, J., Ajjarapu, V., Andersson, G., Bose, A., Canizares, C., Hatziargyriou, N., Hill, D., Stankovic, A., Taylor, C., et al. (2004). Definition and classification of power system stability IEEE/CIGRE joint task force on stability terms and definitions. *Power Systems, IEEE Transactions on*, 19(3):1387–1401.

Leelaruji, R., Vanfretti, L., and Almas, M. S. (2012). Voltage stability monitoring using sensitivities computed from synchronized phasor measurement data. In *Power and Energy Society General Meeting, 2012 IEEE*, pages 1–8. IEEE.

Li, W., Chen, T., and Xu, W. (2010). On impedance matching and maximum power transfer. *Electric power systems research*, 80(9):1082–1088.

Lof, P.-A., Andersson, G., and Hill, D. (1993). Voltage stability indices for stressed power systems. *Power Systems, IEEE Transactions on*, 8(1):326–335.

Lof, P.-A., Smed, T., Andersson, G., and Hill, D. (1992). Fast calculation of a voltage stability index. *Power Systems, IEEE Transactions on*, 7(1):54–64.

Milano, F. (2009). Continuous newton's method for power flow analysis. *Power Systems, IEEE Transactions on*, 24(1):50–57.

Milosevic, B. and Begovic, M. (2003). Voltage-stability protection and control using a wide-area network of phasor measurements. *Power Systems, IEEE Transactions on*, 18(1):121–127.

Morison, G., Gao, B., and Kundur, P. (1993). Voltage stability analysis using static and dynamic approaches. *Power Systems, IEEE Transactions on*, 8(3):1159–1171.

Nedic, D. (2002). Tap adjustment in ac load flow. *UMIST, Sept*.

Obadina, O. and Berg, G. (1988). Determination of voltage stability limit in multimachine power systems. *Power Systems, IEEE Transactions on*, 3(4):1545–1554.

ONS (2014). *Procedimentos de Rede*. `http://www.ons.org.br/procedimentos/index.aspxaccessed`, accessed 2015-01-21.

Ordacgi Filho, J. (2010). Brazilian blackout 2009. *PAC World, March*.

Overbye, T. J. (1994). A power flow measure for unsolvable cases. *Power Systems, IEEE Transactions on*, 9(3):1359–1365.

Pal, M. (1994). Modeling and identification of nonlinear dynamic loads in power-systems-discussion.

Pareto, V. (1964). *Cours d'économie politique*. Librairie Droz, ISBN: 978-2600040143.

Parniani, M., Chow, J. H., Vanfretti, L., Bhargava, B., and Salazar, A. (2006). Voltage stability analysis of a multiple-infeed load center using phasor measurement data. In *Power Systems Conference and Exposition, 2006. PSCE'06. 2006 IEEE PES*, pages 1299–1305. IEEE.

Peng, J.-H., Sherry, R., and Nair, N.-K. (2011). Phasor measurement network and its applications in the new zealand grid: Overview and experiences. In *Power and Energy Society General Meeting, 2011 IEEE*, pages 1–8. IEEE.

Phadke, A. G. (2002). Synchronized phasor measurements-a historical overview. In *Transmission and Distribution Conference and Exhibition 2002: Asia Pacific. IEEE/PES*, volume 1, pages 476–479. IEEE.

Pinto, C. M., Lopes, A. M., and Machado, J. T. (2012). A review of power laws in real life phenomena. *Communications in Nonlinear Science and Numerical Simulation*, 17(9):3558–3578.

Press, W., Flannery, B., Teukolsky, S., and Vetterling, W. (1992). *Numerical Recipes in C: The Art of Scientific Computing, Second Edition*. Cambridge University Press, ISBN 978-0521431088.

Price, W., Chiang, H.-D., Clark, H., Concordia, C., Lee, D., Hsu, J., Ihara, S., King, C., Lin, C., Mansour, Y., et al. (1993). Load representation for dynamic performance analysis. *IEEE Transactions on Power Systems*, 8(2):472–482.

Repo, S. . (2001). *On-line voltage stability assessment of power systems - An approach of black-box modeling*. PhD thesis, Tampere University of Technology.

Romero Navarro, I. (2002). *Dynamic Load Models for Power Systems-Estimation of Time-Varying Parameters During Normal Operation*, volume 1034. Dept. of Industrial Electrical Engineering and Automation, Lund Institute of Technology, ISBN 91-88934-26-8.

Smon, I., Verbic, G., and Gubina, F. (2006). Local voltage-stability index using Tellegen's theorem. *Power Systems, IEEE Transactions on*, 21(3):1267–1275.

Su, H.-Y., Chou, Y.-T., and Liu, C.-W. (2012). Estimation of voltage stability margin using synchrophasors. In *Power and Energy Society General Meeting, 2012 IEEE*, pages 1–7. IEEE.

Tate, J. E. and Overbye, T. J. (2005). A comparison of the optimal multiplier in polar and rectangular coordinates. *Power Systems, IEEE Transactions on*, 20(4):1667–1674.

Tavares, B., Bedriñana, M., and Castro, C. A. (2011). Practical method for computing the maximum loading point using a load flow with step size optimisation. *IET generation, transmission & distribution*, 5(12):1250–1258.

Tavares, B. L., Bedriñana, M. F., and Castro, C. A. (2009). New method based on load flow with step size optimization for calculating the maximum loading point. In *PowerTech, 2009 IEEE Bucharest*, pages 1–7. IEEE.

Tavares, B. L., Bedriñana, M. F., and Castro, C. A. (2010). Practical method for computing the maximum loading point based on load flow with step size optimization. In *Power and Energy Society General Meeting, 2010 IEEE*, pages 1–8. IEEE.

Tchokonte, Y. N. N. (2009). *Real-time identification and monitoring of the voltage stability margin in electric power transmission systems using synchronized phasor measurements*. PhD thesis, University of Kassel.

Tiranuchit, A. and Thomas, R. (1988). A posturing strategy against voltage instabilities in electric power systems. *Power Systems, IEEE Transactions on*, 3(1):87–93.

Trias, A. (2012). The holomorphic embedding load flow method. In *Power and Energy Society General Meeting, 2012 IEEE*, pages 1–8. IEEE.

Tuan, T., Fandino, J., Hadjsaid, N., Sabonnadiere, J., and Vu, H. (1994). Emergency load shedding to avoid risks of voltage instability using indicators. *Power Systems, IEEE Transactions on*, 9(1):341–351.

Van Cutsem, T. (2000). Voltage instability: phenomena, countermeasures, and analysis methods. *Proceedings of the IEEE*, 88(2):208–227.

Van Cutsem, T. and Vournas, C. (1998). *Voltage stability of electric power systems*, volume 441. Springer, ISBN:978-0792381396.

Verbic, G. and Gubina, F. (2002). A novel concept for voltage collapse protection based on local phasors. In *Transmission and Distribution Conference and Exhibition 2002: Asia Pacific. IEEE/-PES*, volume 1, pages 124–129. IEEE.

Verbic, G. and Gubina, F. (2004). A new concept of voltage-collapse protection based on local phasors. *IEEE TRANSACTIONS ON POWER DELIVERY*, 19(2):576–581.

Vournas, C. D. and Van Cutsem, T. (2008). Local identification of voltage emergency situations. *Power Systems, IEEE Transactions on*, 23(3):1239–1248.

Vu, K., Begovic, M. M., Novosel, D., and Saha, M. M. (1999). Use of local measurements to estimate voltage-stability margin. *Power Systems, IEEE Transactions on*, 14(3):1029–1035.

Wang, X., Ejebe, G., Tong, J., and Waight, J. (1998). Preventive/corrective control for voltage stability using direct interior point method. *Power Systems, IEEE Transactions on*, 13(3):878–883.

Warland, L. and Holen, A. T. (2001). A voltage instability predictor using local area measurements (vip++). In *Power Tech Proceedings, 2001 IEEE Porto*, volume 2, pages 6–pp. IEEE.

Xavier, C. E. (2013). Contribution to the calculation of the maximum loading point on power systems. Master's thesis, State University of Campinas.

Xavier, C. E., Bedrinana, M. F., and Castro, C. A. (2013). Robust computation of voltage stability margins for transmission and distribution grids. In *Power and Energy Society General Meeting (PES), 2013 IEEE*, pages 1–5. IEEE.

Yang, J.-Z. and Liu, C.-W. (2000). A precise calculation of power system frequency and phasor. *Power Delivery, IEEE Transactions on*, 15(2):494–499.

Yoshida, H., Kawata, K., Fukuyama, Y., Takayama, S., and Nakanishi, Y. (2000). A particle swarm optimization for reactive power and voltage control considering voltage security assessment. *Power Systems, IEEE Transactions on*, 15(4):1232–1239.

Zarate, L., Castro, C. A., Ramos, J. L. M., and Ramos, E. R. (2006). Fast computation of voltage stability security margins using nonlinear programming techniques. *Power Systems, IEEE Transactions on*, 21(1):19–27.

Zima, M., Larsson, M., Korba, P., Rehtanz, C., and Andersson, G. (2005). Design aspects for wide-area monitoring and control systems. *Proceedings of the IEEE*, 93(5):980–996.